A QCD PRIMER

G. Altarelli
CERN, Geneva, Switzerland

Contents

1 INTRODUCTION **65**

2 MASSLESS QCD AND SCALE INVARIANCE **70**

3 THE RENORMALISATION GROUP AND ASYMPTOTIC FREEDOM **73**

4 MORE ON THE RUNNING COUPLING **78**

5 APPLICATION TO HARD PROCESSES **79**
5.1 $R_{e^+e^-}$ and Related Processes 79
5.2 The Final State in e^+e^- Annihilation 82
5.3 Deep Inelastic Scattering 83
5.4 Factorisation and the QCD Improved Parton Model 89

6 MEASUREMENTS OF α_s **95**
6.1 α_s from e^+e^- colliders 95
6.2 α_s from Deep Inelastic Scattering 96

7 CONCLUSION **98**

8 APPENDIX: The Formalism of Gauge Theories **99**

1 INTRODUCTION

These four lectures are devoted to an elementary introduction to Quantum Chromo-Dynamics (QCD), the theory of strong interactions. Four lectures are not much. So after a general introduction I will concentrate on the basic principles and the main applications of perturbative QCD (for reviews of the subject see for example [1], [2], [3]). I will try to put the main emphasis on ideas with only a minimum of technicalities.

At present most of particle physics is well understood in terms of the Standard Model (SM), which is a gauge theory of strong and electroweak interactions based on the group $SU(3) \bigotimes SU(2) \bigotimes U(1)_Y$. The $SU(3)$ factor is the colour group of QCD, while $SU(2) \bigotimes U(1)_Y$ is the Glashow-Weinberg-Salam electroweak symmetry group. The electroweak symmetry is spontaneously broken down to $U(1)_Q$, the phase group of the electric charge Q_e (that is, Q is the charge operator in units of e, the proton charge), different from the $U(1)_Y$ of weak hypercharge: $Q = t_3 + Y/2$, where t_3 is the third component of the weak isospin generator of $SU(2)$. The group $SU(3) \bigotimes U(1)_Q$ is believed to be an exact gauge symmetry of nature. The corresponding gauge bosons, the eight gluons and the photon are massless. Matter fields include three families of coloured quarks and colourless leptons. Quarks and gluons (q and g) are the fields that have strong interactions described by QCD. The statement that QCD is a gauge theory based on the

group $SU(3)$ with colour triplet quark matter fields fixes the QCD lagrangian density to be (a summary of the general formalism of gauge theories is presented in Appendix):

$$\mathcal{L} \;=\; -\frac{1}{4}\sum_{A=1}^{8} F^{A\mu\nu}F^{A}_{\mu\nu} \;+\; \sum_{j=1}^{n_f}\bar{q}_j(i\not{D} - m_j)q_j \tag{1}$$

Here: q_j are the quark fields (of n_f different flavours) with mass m_j; $\not{D} = D_\mu\gamma^\mu$, where γ^μ are the Dirac matrices and D_μ is the covariant derivative:

$$D_\mu = \partial_\mu - ie_s\mathbf{g}_\mu; \tag{2}$$

e_s is the gauge coupling, later we will mostly use, in analogy with QED

$$\alpha_s = \frac{e_s^2}{4\pi}; \tag{3}$$

$\mathbf{g}_\mu = \sum_A \; t^A g^A_\mu$ where g^A_μ, $A = 1, 8$, are the gluon fields and t^A are the $SU(3)$ group generators in the triplet representation of quarks (i.e. t_A are 3x3 matrices acting on q); the generators obey the commutation relations $[t^A, t^B] = iC_{ABC}t^C$ where C_{ABC} are the complete antisymmetric structure constants of $SU(3)$ (the normalisation of C_{ABC} and of e_s is specified by $Tr[t^A t^B] = \delta^{AB}/2$);

$$F^A_{\mu\nu} \;=\; \partial_\mu g^A_\nu - \partial_\nu g^A_\mu \;-\; e_s C_{ABC} g^B_\mu g^C_\nu \tag{4}$$

The Feynman rules of QCD are listed in Fig 1. The physical vertices in QCD include the gluon-quark-antiquark vertex, analogous to the QED photon-fermion-antifermion coupling, but also the 3-gluon and 4-gluon vertices, of order e_s and e_s^2 respectively, which have no analogue in an abelian theory like QED. In fact the QED lagrangian density is given by:

$$\mathcal{L} \;=\; -\frac{1}{4}F^{\mu\nu}F_{\mu\nu} \;+\; \sum_{\psi}\bar{\psi}(i\not{D} - m_\psi)\psi \tag{5}$$

with the covariant derivative given in terms of the photon field A_μ and the charge operator Q by:

$$D_\mu = \partial_\mu - ieA_\mu Q \tag{6}$$

and

$$F_{\mu\nu} \;=\; \partial_\mu A_\nu - \partial_\nu A_\mu \tag{7}$$

In QED the photon is coupled to all electrically charged particles but itself is neutral. In QCD the gluons are coloured hence self-coupled. This is reflected in the fact that in QED $F_{\mu\nu}$ is linear in the gauge field, so that the term $F^2_{\mu\nu}$ in the lagrangian is a pure kinetic term, while in QCD $F^A_{\mu\nu}$ is quadratic in the gauge field so that in $F^{A2}_{\mu\nu}$ we find cubic and quartic vertices beyond the kinetic term. Also instructive is to consider the case of scalar QED:

$$\mathcal{L} \;=\; -\frac{1}{4}F^{\mu\nu}F_{\mu\nu} \;+\; (D_\mu\phi)^\dagger(D^\mu\phi) - m^2(\phi^\dagger\phi) \tag{8}$$

For $Q = 1$ we have:

$$(D_\mu\phi)^\dagger(D^\mu\phi) \;=\; (\partial_\mu\phi)^\dagger(\partial^\mu\phi) \;+\; ieA_\mu[(\partial^\mu\phi)^\dagger\phi \;-\; \phi^\dagger(\partial^\mu\phi)] \;+\; e^2A_\mu A^\mu\phi^\dagger\phi \tag{9}$$

We see that for a charged boson in QED, given that the kinetic term for bosons is quadratic in the derivative, there is a two-gauge vertex of order e^2. Thus in QCD the 3-gluon vertex is there because the gluon is coloured and the 4-gluon vertex because the gluon is a boson.

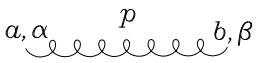

$$= \delta^{ab} \frac{-i\, g^{\alpha\beta}}{p^2 + i\epsilon} \quad \text{(Feynman gauge)}$$

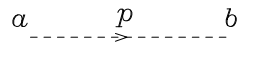

$$= \delta^{ab} \frac{i}{p^2 + i\epsilon}$$

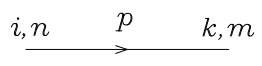

$$= \delta^{ik} \left. \frac{i}{\not{p} - m + i\epsilon} \right|_{mn}$$

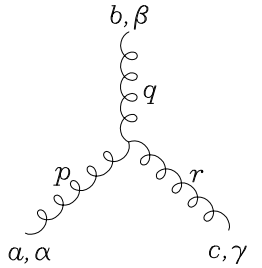

$$= g f^{abc} \left[g^{\alpha\beta}(p-q)^\gamma + g^{\beta\gamma}(q-r)^\alpha + g^{\gamma\alpha}(r-p)^\beta \right]$$

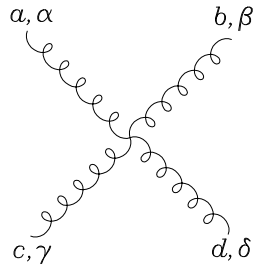

$$\begin{aligned} = \; & -ig^2 f^{xac} f^{xbd} \left(g^{\alpha\beta} g^{\gamma\delta} - g^{\alpha\delta} g^{\beta\gamma} \right) \\ & -ig^2 f^{xad} f^{xbc} \left(g^{\alpha\beta} g^{\gamma\delta} - g^{\alpha\gamma} g^{\beta\delta} \right) \\ & -ig^2 f^{xab} f^{xcd} \left(g^{\alpha\gamma} g^{\beta\delta} - g^{\alpha\delta} g^{\beta\gamma} \right) \end{aligned}$$

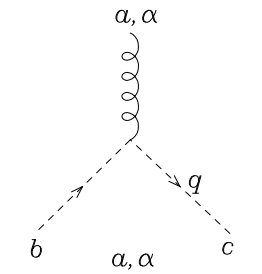

$$= -g f^{abc}\, q^\alpha$$

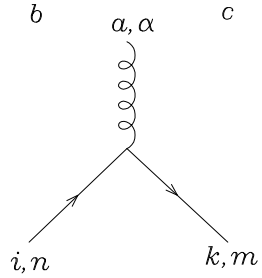

$$= ig\, \lambda^a_{ki}\, \gamma^\alpha_{mn}$$

Fig. 1: Feynman rules for QCD. The solid lines represent the femions, the curly lines the gluons, and the dotted lines represent the ghosts.

The QCD lagrangian in eq.(1) has a simple structure but a very rich dynamical content. It gives rise to a complex spectrum of hadrons, it implies the striking properties of confinement and asymptotic freedom, is endowed with an approximate chiral symmetry which is spontaneously broken, has a highly non trivial topological vacuum structure (instantons, $U(1)_A$ symmetry breaking, strong CP violation (?)...), an intriguing phase transition diagram (colour deconfinement, quark-gluon plasma, chiral symmetry restauration, colour superconductivity, ...).

Confinement is the property that no isolated coloured charge can exist but only colour singlet particles. For example, the potential between a quark and an antiquark has been studied on the lattice and it has a Coulomb part at short distances and a linearly rising term at long distances:

$$V_{q\bar{q}} \approx C_F[\frac{\alpha_s(r)}{r} + ... + \sigma r] \tag{10}$$

where

$$\mathbf{1}_3 \; C_F = \sum_A t^A t^A = \frac{N_C^2 - 1}{2N_C} \; \mathbf{1}_3 \tag{11}$$

with N_C the number of colours ($N_C = 3$ in QCD). The scale dependence of α_s (the distance r is Fourier-conjugated to momentum transfer) will be explained in detail in this course. The linearly rising term makes it energetically impossible to separate a $q - \bar{q}$ pair. If the pair is created at one space-time point, for example in e^+e^- annihilation, and then the quark and the antiquark start moving away from each other in the center of mass frame, it soon becomes energetically favourable to create additional pairs, smoothly distributed in rapidity between the two leading charges, which neutralise colour and allow the final state to be reorganised into two jets of colourless hadrons, that communicate in the central region by a number of "wee" hadrons with small energy. It is just like the familiar example of the broken magnet: if you try to isolate a magnetic pole by stretching a dipole, the magnet breaks down and two new poles appear at the breaking point. Very often in QCD one computes inclusive rates for partons (the fields in the lagrangian, that is, in QCD, quarks and gluons) and takes them as equal to rates for hadrons. Partons and hadrons are considered as two equivalent sets of complete states. This is called "global duality" and it is rather safe in the rare instance of a totally inclusive final state. It is less so for distributions, like distributions in the invariant mass M ("local duality") where it can be reliable only if smeared over a sufficiently wide bin in M.

Confinement is essential to explain why nuclear forces have very short range while massless gluon exchange would be long range. Nucleons are colour singlets and they cannot exchange colour octet gluons but only colourless states. The lightest colour singlet hadronic particles are pions. So the range of nuclear forces is fixed by the pion mass $r \simeq m_\pi^{-1} \simeq 10^{-13}$ cm : $V \approx \exp(-m_\pi r)/r$.

Why $SU(N_C = 3)_{colour}$? The selection of $SU(3)$ as colour gauge group is unique in view of a number of constraints. (a) The group must admit complex representations because it must be able to distinguish a quark from an antiquark. In fact there are meson states made up of $q\bar{q}$ but not analogous qq bound states. Among simple groups this restricts the choice to $SU(N)$ with $N \geq 3$, $SO(4N + 2)$ with $N \geq 2$ (taking into account that $SO(6)$ has the same algebra as $SU(4)$) and $E(6)$. (b) The group must admit a completely antisymmetric colour singlet baryon made up of 3 quarks: qqq. From the study of hadron spectroscopy we know that the low lying baryons, completing an octet and a decuplet of (flavour) $SU(3)$ (the approximate symmetry that rotate the 3 light quarks u, d and s), are made up of three quarks and are colour singlets. The qqq wave function must be completely antisymmetric in colour in order to agree with Fermi statistics. Indeed if we consider, for example, a N^{*++} with spin z-component $+3/2$, this is made up of $(u \Uparrow u \Uparrow u \Uparrow)$ in an s-state. Thus its wave function is totally symmetric in space, spin and flavour so that complete antisymmetry in colour is required by Fermi statistics. In

QCD this requirement is very simply satisfied by $\epsilon_{abc}q^a q^b q^c$ where a, b, c are $SU(3)_{colour}$ indices. (c) The choice of $SU(N_C = 3)_{colour}$ is confirmed by many processes that directly measure N_C. Some examples are listed here. The total rate for hadronic production in e^+e^- annihilation is linear in N_C. Precisely if we consider $R = \sigma(e^+e^- \to hadrons)/\sigma_{point}(e^+e^- \to \mu^+\mu^-)$ above $b\bar{b}$ threshold and below m_Z and we neglect small computable radiative corrections (that will be discussed later) we have a sum of individual contributions (proportional to Q^2) from $q\bar{q}$ final states with $q = u,\ c,\ d,\ s,\ b$:

$$R \ \approx \ N_C[2 \cdot \frac{4}{9} \ + \ 3 \cdot \frac{1}{9}] \ \approx \ N_C \frac{11}{9} \tag{12}$$

The data neatly indicate $N_C = 3$ as seen from Fig. 2 [4]. The slight excess of the data with respect to the value 11/3 is due to the QCD radiative corrections. Similarly we can consider the branching ratio $B(W^- \to e^-\bar{\nu})$, again in Born approximation. The possible fermion-antifermion $(f\bar{f})$ final states are for $f = e^-,\ \mu^-,\ \tau^-, d, s$ (there is no $f = b$ because the top quark is too heavy for $b\bar{t}$ to occur). Each channel gives the same contribution, except that for quarks we have N_C colours:

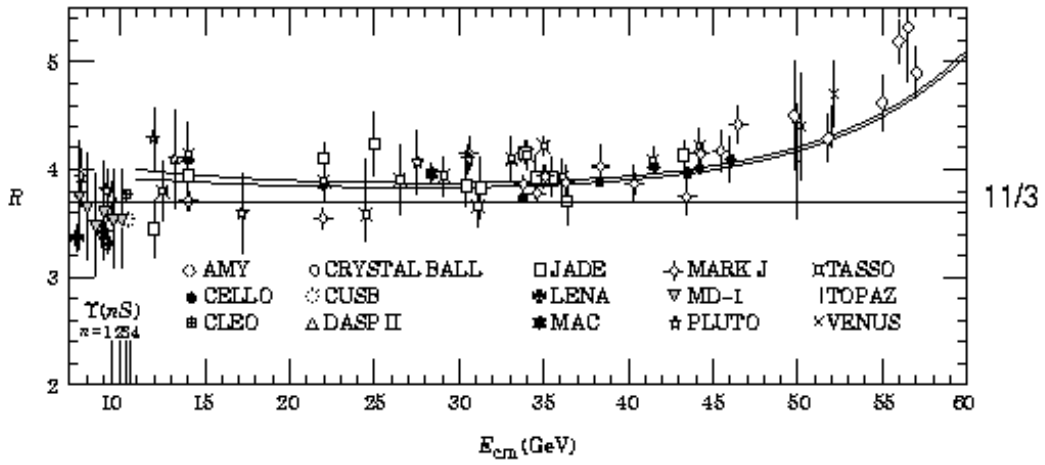

Fig. 2:

$$B(W^- \to e^-\bar{\nu}) \ \approx \ \frac{1}{3 + 2N_C} \tag{13}$$

For $N_C = 3$ we obtain $B = 11\%$ and the experimental number is $B = 10.7\%$. Another analogous example is the branching ratio $B(\tau^- \to e^-\bar{\nu}_e\nu_\tau)$. From the final state channels with $f = e^-,\ \mu^-,\ d$ we find

$$B(\tau^- \to e^-\bar{\nu}_e\nu_\tau) \ \approx \ \frac{1}{2 + N_C} \tag{14}$$

For $N_C = 3$ we obtain $B = 20\%$ and the experimental number is $B = 18\%$ (the less accuracy in this case is explained by the larger radiative and phase-space corrections because the mass of τ^- is much smaller than m_W). An important process that is quadratic in N_C is the rate $\Gamma(\pi^0 \to 2\gamma)$. This rate can be reliably calculated from a solid theorem in field theory which has to do with the chiral anomaly:

$$\Gamma(\pi^0 \to 2\gamma) \approx \ (\frac{N_C}{3})^2 \frac{\alpha^2 m_{\pi^0}^3}{32\pi^3 f_\pi^2} \ = \ (7.73 \pm 0.04)(\frac{N_C}{3})^2 \ eV \tag{15}$$

where the prediction is obtained for $f_\pi = (130.7 \pm 0.37)\ MeV$. The experimental result is $\Gamma = (7.7 \pm 0.5)\ eV$ in remarkable agreement with $N_C = 3$. There are many more experimental confirmations that $N_C = 3$: for example the rate for Drell-Yan processes (see section 5.4) is inversely proportional to N_C.

How do we get testable predictions from QCD? On the one hand there are non perturbative methods. The most important at present is the technique of lattice simulations: it is based on first principles, it has produced very valuable results on confinement, phase transitions, bound states, hadronic matrix elements and so on, and it is by now an established basic tool. The main limitation is computing power and therefore there is continuous progress and a lot of good perspectives for the future. Another class of approaches is based on effective lagrangians which provide simpler approximations than the full theory, valid in some definite domain of physical conditions. Chiral lagrangians are based on soft pion theorems and are valid for suitable processes at energies below 1 GeV. Heavy quark effective theories are obtained from expanding in inverse powers of the heavy quark mass and are mainly important for the study of b and, to less accuracy, c decays. The approach of QCD sum rules has led to interesting results but appears to offer not much potential for further development. Similarly specific potential models for quarkonium have a limited range of application. On the other hand, the perturbative approach, based on asymptotic freedom, still remains the main quantitative connection to experiment, due to its wide range of applicability to all sorts of "hard" processes. Perturbative QCD will be the main subject in the following. I will discuss its foundations and main applications in the next sections.

2 MASSLESS QCD AND SCALE INVARIANCE

The QCD lagrangian in eq.(1) only specifies the theory at the classical level. The procedure for quantisation of gauge theories involves a number of complications that arise from the fact that not all degrees of freedom of gauge fields are physical because of the constraints from gauge invariance which can be used to eliminate the dependent variables. This is already true for abelian theories and we are familiar with the QED case. One introduces a gauge fixing term (an additional term in the lagrangian density that acts as a Lagrange multiplier in the action extremisation). One can choose to preserve manifest Lorentz invariance. In this case, one adopts a covariant gauge, like the Lorentz gauge, and in QED one proceeds according to the formalism of Gupta-Bleuler. Or one can give up explicit formal covariance and work in a non covariant gauge, like the Coulomb or the axial gauges, and only quantise the physical degrees of freedom (the transverse components of the photon field). While this is all for an abelian gauge theory, in the non-abelian case some additional complications arise, in particular the necessity to introduce ghosts for the formulation of Feynman rules. There are in general as many ghost fields as gauge bosons and they appear in the form of a transformation Jacobian in the Feynman diagram functional integral. Ghosts only propagate in closed loops and their vertices with gluons can be included as additional terms in the lagrangian density which are fixed once the gauge fixing terms and their infinitesimal gauge transformations are specified. We skip the detailed derivation of the complete Feynman rules in a given gauge as they appear in Fig 1.

Once the Feynman rules are derived we have a formal perturbative expansion but loop diagrams generate infinities. First a regularisation must be introduced, compatible with gauge symmetry and Lorentz invariance. This is possible in QCD. In principle one can introduce a cut-off Λ (with dimensions of energy), for example, a' la Pauli-Villars. But at present the universally adopted regularisation procedure is dimensional regularisation that we will briefly describe later on. After regularisation the next step is renormalisation. In a renormalisable theory (like for all gauge theories in 4 spacetime dimensions and for QCD in particular) the dependence on the cutoff can be completely reabsorbed in a redefinition of particle masses, of gauge coupling(s) and

of wave function normalisations. After renormalisation is achieved the perturbative definition of the quantum theory that corresponds to a classical lagrangian like in eq.(1) is completed.

In the QCD Lagrangian of eq.(1) quark masses are the only parameters with physical dimensions (we work in the natural system of units $\hbar = c = 1$). Naively we would expect that massless QCD is scale invariant. This is actually true at the classical level. Scale invariance implies that dimensionless observables should not depend on the absolute scale of energy but only on ratios of energy-dimensional variables. The massless limit should be relevant for the asymptotic large energy limit of processes which are non singular for $m \to 0$.

The naive expectation that massless QCD should be scale invariant is false in the quantum theory. The scale symmetry of the classical theory is unavoidably destroyed by the regularisation and renormalisation procedure which introduce a dimensional parameter in the quantum version of the theory. When a symmetry of the classical theory is necessarily destroyed by quantisation, regularisation and renormalisation one talks of an "anomaly". So, in this sense, scale invariance in massless QCD is anomalous.

While massless QCD is finally not scale invariant, the departures from scaling are asymptotically small, logarithmic and computable. In massive QCD there are additional mass corrections suppressed by powers of m over the energy scale (for non singular processes in the limit $m \to 0$). At the parton level (q and g) we can conceive to apply the asymptotics from massless QCD to processes and observables (we use the word "processes" for both) with the following properties ("hard processes"). (a) All relevant energy variables must be large:

$$E_i \;=\; z_i Q, \qquad\qquad Q >> m_j; \qquad\qquad z_i\text{: scaling variables o(1)} \tag{16}$$

(b) There should be no infrared singularities (one talks of "infrared safe" processes). (c) The processes concerned must be finite for $m \to 0$ (no mass singularities). To possibly satisfy these criteria processes must be as "inclusive" as possible: one should include all final states with massless gluon emission and add all mass degenerate final states (given that quarks are massless also $q - \bar{q}$ pairs can be massless if "collinear", that is moving together in the same direction at the common speed of light).

Let us discuss more in detail infrared and collinear safety. Consider, for example, a quark virtual line that ends up into a real quark plus a real gluon (Fig. 3).

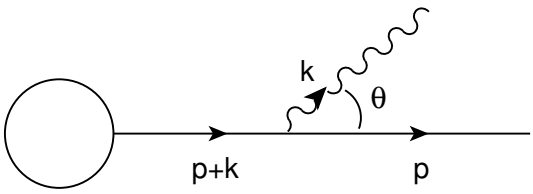

Fig. 3:

For the propagator we have:

$$\text{propagator} \;=\; \frac{1}{(\mathrm{p}+\mathrm{k})^2 - \mathrm{m}^2} \;=\; \frac{1}{2(\mathrm{p}\cdot\mathrm{k})} \;=\; \frac{1}{2\mathrm{E_k E_p}} \cdot \frac{1}{1-\beta_\mathrm{p}\cos\theta} \tag{17}$$

Since the gluon is massless, E_k can vanish and this corresponds to an infrared singularity. Remember that we have to take the square of the amplitude and integrate over the final state phase space, or all together, dE_k/E_k. So we get $1/E_k^2$ from the squared amplitude and $d^3k/E_k \sim E_k dE_k$ from the phase space. Also, for $m \to 0$, $\beta_p = \sqrt{1 - m^2/E_p^2} \to 1$ and $(1-\beta_p \cos\theta)$ vanishes at $\cos\theta = 1$. This leads to a collinear mass singularity.

There are two very important theorems on infrared and mass singularities. The first one is the Bloch-Nordsieck theorem: infrared singularities cancel between real and virtual diagrams (see Fig. 4) when all resolution indistinguishable final states are added up. For example, for each real detector there is a minimum energy of gluon radiation that can be detected. For the cancellation of infrared divergences, one should add all possible gluon emission with a total energy below the detectable minimum. The second one is the Kinoshita-Lee-Nauenberg theorem: mass singularities connected with an external particle of mass m are canceled if all degenerate states (that is with the same mass) are summed up. That is for a final state particle of mass m we should add all final states that in the limit $m \to 0$ have the same mass, also including gluons and massless pairs. If a completely inclusive final state is taken, only the mass singularities from the initial state particles remain (we shall see that they will be absorbed inside the non perturbative parton densities, which are probability densities of finding the given parton in the initial hadron).

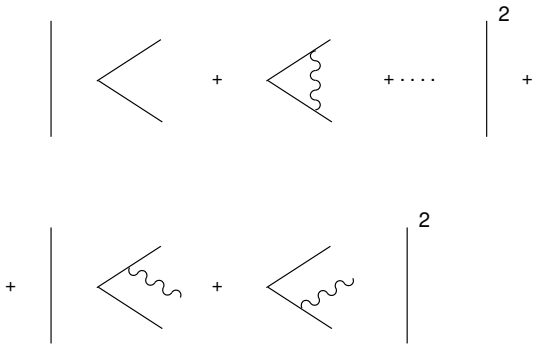

Fig. 4:

Hard processes to which the massless QCD asymptotics can possibly apply must be infrared and collinear safe, that is must satisfy the requirements from the Bloch-Nordsieck and the Kinoshita-Lee-Nauenberg theorems. We give now some examples of important hard processes. One of the simplest hard processes is the totally inclusive cross section for hadron production in e^+e^- annihilation, Fig. 5, parameterised in terms of the already mentioned dimensionless observable $R = \sigma(e^+e^- \to hadrons)/\sigma_{point}(e^+e^- \to \mu^+\mu^-)$. The pointlike cross section in the denominator is given by $\sigma_{point} = 4\pi\alpha^2/3s$, where $s = Q^2 = 4E^2$ is the squared total center of mass energy and Q is the mass of the exchanged virtual gauge boson. At parton level the final state is $(q\bar{q} \ + \ n \ g \ + \ n' \ q'\bar{q}')$ and n and n' are limited at each order of perturbation theory. It is assumed that the conversion of partons into hadrons does not affect the rate (it happens with probability 1). We have already mentioned that in order for this to be true within a given accuracy an averaging over a sufficiently large bin of Q must be understood. The binning width is larger in the vicinity of thresholds: for example when one goes across the charm $c\bar{c}$ threshold the physical cross-section shows resonance bumps which are absent in the smooth partonic counterpart which however gives an average of the cross-section.

A very important class of hard processes is Deep Inelastic Scattering (DIS)

$$l \ + \ N \to l' \ + \ X \qquad\qquad l = e^{\pm}, \mu^{\pm}, \nu, \bar{\nu} \tag{18}$$

which has played and still plays a very important role for our understanding of QCD and of nucleon structure. For the processes in eq.(18), shown in Fig 6, we have, in the lab system where the nucleon of mass m is at rest:

$$Q^2 \ = \ -q^2 \ = \ -(k-k')^2 \ = \ 4EE' \sin^2\theta/2; \qquad m\nu \ = \ (p.q); \qquad x \ = \ \frac{Q^2}{2m\nu} \tag{19}$$

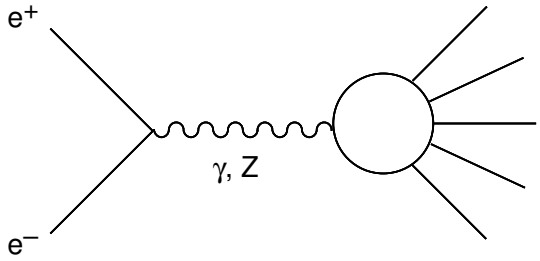

Fig. 5:

In this case the virtual momentum q of the gauge boson is spacelike. x is the familiar Bjorken variable.

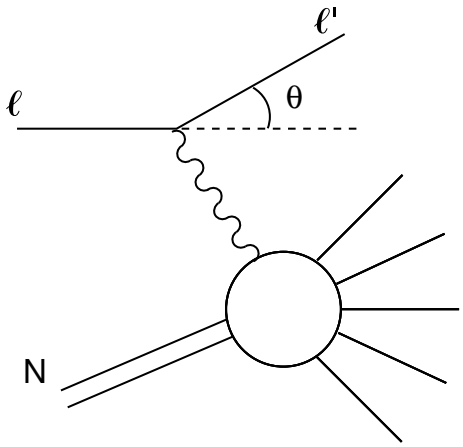

Fig. 6:

3 THE RENORMALISATION GROUP AND ASYMPTOTIC FREEDOM

In this section we aim at providing a reasonably detailed introduction to the renormalisation group formalism and the concept of running coupling which leads to the result that QCD has the property of asymptotic freedom. We start with a summary on how renormalisation works.

In the simplest conceptual situation imagine that we implement regularisation of divergent integrals by introducing a dimensional cut-off Λ that respects gauge and Lorentz invariance. The dependence of renormalised quantities on Λ is eliminated by absorbing it into a redefinition of m (the quark mass: for simplicity we assume a single flavour here), the gauge coupling e (can be e in QED or e_s in QCD) and the wave function renormalisation factors $Z_{q,g}^{1/2}$ for q and g, using suitable renormalisation conditions (that is precise definitions of m, g and Z). For example we can define the renormalised mass m as the position of the pole in the quark propagator and, similarly, the normalisation Z_q as the residue at the pole:

$$\text{Propagator} \;=\; \frac{\mathrm{Z_q}}{\mathrm{p^2 - m^2}} \;+\; \mathrm{no-pole\ terms} \tag{20}$$

The renormalised coupling e can be defined in terms of a renormalised 3-point vertex at some specified values of the external momenta. We now become more specific by concentrating in the case of massless QCD. If we start from a vanishing mass at the classical (or "bare") level,

$m_0 = 0$, the mass is not renormalised because it is protected by a symmetry, chiral symmetry. The conserved currents of chiral symmetry are axial currents: $\bar{q}\gamma_\mu\gamma_5 q$. The divergence of the axial current gives, by using the Dirac equation, $\partial^\mu(\bar{q}\gamma_\mu\gamma_5 q) = 2m\bar{q}\gamma_5 q$. So the axial current and corresponding axial charge are conserved in the massless limit. Since QCD is a vector theory we have not to worry about chiral anomalies in this respect. So one can choose a regularisation that preserves chiral symmetry besides gauge and Lorentz symmetry. Then the renormalised mass remains zero. The renormalised propagator has the form in eq.(20) with $m = 0$.

The renormalised coupling e_s can be defined from the renormalised 3-gluon vertex at a scale $-\mu^2$ (Fig. 7):

$$V_{bare}(p^2, q^2, r^2) = ZV_{ren}(p^2, q^2, r^2), \qquad Z = Z_g^{3/2} Z_V, \qquad e_s = V_{ren}(-\mu^2, -\mu^2, -\mu^2) \tag{21}$$

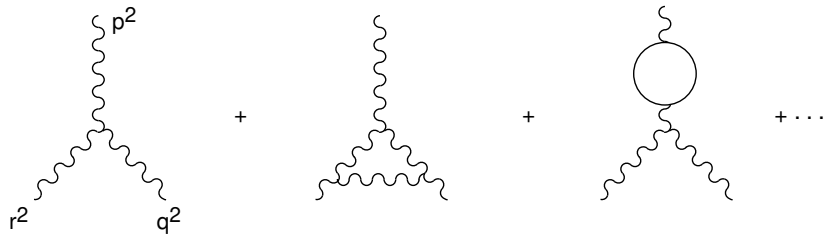

Fig. 7:

Here V_{bare} is what is obtained from computing the Feynman diagrams including, for example, the 1-loop corrections at the lowest non trivial order (V_{bare} is defined so that it coincides with e_{s0} in lowest order). It contains the cut-off Λ but does not know μ. Z is a factor that depends on the cut-off. Because of infrared singularities the defining scale μ cannot vanish. The negative value $-\mu^2 < 0$ is chosen to stay away from physical cuts (a gluon with negative virtual mass cannot decay). Similarly we can define Z_g from the massless gluon propagator at the same scale $-\mu^2$ (the vanishing mass of the gluon is guaranteed by gauge invariance).

After computing all 1-loop diagrams in Fig. 7 we have:

$$\begin{aligned} V_{bare}(p^2, p^2, p^2) &= e_{0s}[1 + c\alpha_{0s} \cdot \log\frac{\Lambda^2}{p^2} + ...] = \\ &= [1 + c\alpha_s \cdot \log\frac{\Lambda^2}{-\mu^2} + ...]e_s[1 + c\alpha_s \cdot \log\frac{-\mu^2}{p^2} + ...] = ZV_{ren} \end{aligned} \tag{22}$$

Note the replacement of e_0 with e in the second step. The definition of e_s demands that one precisely specifies what is included in Z. For this, in a given renormalisation scheme, a prescription is fixed to specify the finite terms that go into Z (i.e. the terms of order α_s that accompany $\log\Lambda^2$). Then V_{ren} is specified and the renormalised coupling is defined from it according to eq.(21). For example, in the momentum subtraction scheme we define $V_{ren}(p^2, p^2, p^2) = e_s + V_{bare}(p^2, p^2, p^2) - V_{bare}(-\mu^2, -\mu^2, -\mu^2)$, which is equivalent to say, at 1-loop, that all finite terms that do not vanish at $p^2 = -\mu^2$ are included in Z.

A crucial observation is that V_{bare} depends on Λ but not on μ, which is only introduced when Z, V_{ren} and hence α_s are defined. (From here on, for shorthand, we write α to indicate either the QED coupling or the QCD coupling α_s). More in general for a generic Green function G, we similarly have:

$$G_{bare}(\Lambda^2, \alpha_0, p_i^2) = ZG_{ren}(\mu^2, \alpha, p_i^2) \tag{23}$$

so that we have:

$$\frac{dG_{bare}}{d\log\mu^2} \;=\; \frac{d}{d\log\mu^2}[ZG_{ren}] \;=\; 0 \tag{24}$$

or

$$Z[\frac{\partial}{\partial\log\mu^2} \;+\; \frac{\partial\alpha}{\partial\log\mu^2}\frac{\partial}{\partial\alpha} \;+\; \frac{1}{Z}\frac{\partial Z}{\partial\log\mu^2}]G_{ren} \;=\; 0 \tag{25}$$

Finally the renormalisation group equation (RGE) can be written as:

$$[\frac{\partial}{\partial\log\mu^2} \;+\; \beta(\alpha)\frac{\partial}{\partial\alpha} \;+\; \gamma(\alpha)]G_{ren} \;=\; 0 \tag{26}$$

where

$$\beta(\alpha) \;=\; \frac{\partial\alpha}{\partial\log\mu^2} \tag{27}$$

and

$$\gamma(\alpha) \;=\; \frac{\partial\log Z}{\partial\log\mu^2} \tag{28}$$

Note that $\beta(\alpha)$ does not depend on which Green function G we are considering, but it is a property of the theory and the renormalisation scheme adopted, while $\gamma(\alpha)$ also depends on G.

Assume that we want to apply the RGE to some hard process at a large scale Q, related to a Green function G that we can always take as adimensional (by multiplication by a suitable power of Q). Since the interesting dependence on Q will be logarithmic we introduce the variable t as :

$$t \;=\; \log\frac{Q^2}{\mu^2} \tag{29}$$

Then we can write $G_{ren} \equiv F(t,\alpha,x_i)$ where x_i are scaling variables (we often omit to write them in the following). In the naive scaling limit F should be independent of t. To find the actual dependence on t, we want to solve the RGE

$$[-\frac{\partial}{\partial t} \;+\; \beta(\alpha)\frac{\partial}{\partial\alpha} \;+\; \gamma(\alpha)]G_{ren} \;=\; 0 \tag{30}$$

with a given boundary condition at $t=0$ (or $Q^2=\mu^2$): $F(0,\alpha)$.

We first solve the RGE in the simplest case that $\gamma(\alpha)=0$. This is not an unphysical case: for example, it applies to $R_{e^+e^-}$ where the vanishing of γ is related to the non renormalisation of the electric charge in QCD (otherwise the proton and the electron charge would not exactly compensate: this will be better explained later). So we consider the equation:

$$[-\frac{\partial}{\partial t} \;+\; \beta(\alpha)\frac{\partial}{\partial\alpha}]G_{ren} \;=\; 0 \tag{31}$$

The solution is simply

$$F(t,\alpha) \;=\; F[0,\alpha(t)] \tag{32}$$

where the "running coupling" $\alpha(t)$ is defined by:

$$t \;=\; \int_\alpha^{\alpha(t)} \frac{1}{\beta(\alpha')}d\alpha' \tag{33}$$

Note that from this definition it follows that $\alpha(0) \;=\; \alpha$, so that the boundary condition is also satisfied. To prove that $F[0,\alpha(t)]$ is indeed the solution, we first take derivatives with respect of t and α (the two independent variables) of both sides of eq.(33). By taking d/dt we obtain

$$1 \;=\; \frac{1}{\beta(\alpha(t))}\frac{\partial\alpha(t)}{\partial t} \tag{34}$$

We then take $d/d\alpha$ and obtain

$$0 \;=\; -\frac{1}{\beta(\alpha)} \;+\; \frac{1}{\beta(\alpha(t))}\frac{\partial\alpha(t)}{\partial\alpha} \tag{35}$$

These two relations make explicit the dependence of the running coupling on t and α:

$$\frac{\partial\alpha(t)}{\partial t} \;=\; \beta(\alpha(t)) \tag{36}$$

$$\frac{\partial\alpha(t)}{\partial\alpha} \;=\; \frac{\beta(\alpha(t))}{\beta(\alpha)} \tag{37}$$

Using these two equations one immediately checks that $F[0,\alpha(t)]$ is indeed the solution.

Similarly, one finds that the solution of the more general equation with $\gamma \neq 0$, eq.(30), is given by:

$$F(t,\alpha) \;=\; F[0,\alpha(t)]\exp\int_{\alpha}^{\alpha(t)}\frac{\gamma(\alpha')}{\beta(\alpha')}d\alpha' \tag{38}$$

In fact the sum of the two derivatives acting on the factor $F[0,\alpha(t)]$ vanishes and the exponential is by itself a solution of the complete equation. Note that the boundary condition is also satisfied.

The important point is the appearance of the running coupling that determines the asymptotic departures from scaling. The next step is to study the functional form of the running coupling. From eq.(36) we see that the rate of change with t of the running coupling is determined by the β function. In turn $\beta(\alpha)$ is determined by the μ dependence of the renormalised coupling through eq.(27). Clearly there is no dependence on μ of the basic 3-gluon vertex in lowest order (order e). The dependence starts at 1-loop, that is at order e^3 (one extra gluon has to be emitted and reabsorbed). Thus we obtain that in perturbation theory:

$$\frac{\partial e}{\partial\log\mu^2} \;\propto\; e^3 \tag{39}$$

Recalling that $\alpha \;=\; e^2/4\pi$, we have:

$$\frac{\partial\alpha}{\partial\log\mu^2} \;\propto\; 2e\frac{\partial e}{\partial\log\mu^2} \;\propto\; e^4 \;\propto\alpha^2 \tag{40}$$

Thus the behaviour of $\beta(\alpha)$ in perturbation theory is as follows:

$$\beta(\alpha) \;=\; \pm b\alpha^2[1 \;+\; b'\alpha \;+...] \tag{41}$$

Since the sign of the leading term is crucial in the following discussion, we stipulate that always $b > 0$ and we make the sign explicit in front. By direct calculation at 1-loop one finds:

$$\text{QED}: \qquad \beta(\alpha) \;\sim\; +\,\mathrm{b}\alpha^2 \;+..... \qquad\qquad \mathrm{b} \;=\; \sum_{\mathrm{i}}\frac{\mathrm{N_C}(\mathrm{Q^2})_{\mathrm{i}}}{3\pi} \tag{42}$$

where $N_C = 3$ for quarks and $N_C = 1$ for leptons and the sum runs over all fermions of charge Qe that are coupled. Also, one finds:

$$\text{QCD}: \qquad \beta(\alpha) \;\sim\; -\,\mathrm{b}\alpha^2 \;+..... \qquad\qquad \mathrm{b} \;=\; \frac{11\mathrm{N_C} - 2\mathrm{n_f}}{12\pi} \tag{43}$$

where, as usual, n_f is the number of coupled flavours of quarks (we assume here that $n_f \;\leq\; 16$ so that $b > 0$ in QCD). If $\alpha(t)$ is small we can compute $\beta(\alpha(t))$ in perturbation theory. The sign

in front of b then decides the slope of the coupling: $\alpha(t)$ increases with t (or Q^2) if β is positive at small α (QED), or $\alpha(t)$ decreases with t (or Q^2) if β is negative at small α (QCD). A theory like QCD where the running coupling vanishes asymptotically at large Q^2 is called (ultraviolet) "asymptotically free". An important result that can be proven is that in 4 spacetime dimensions all and only non-abelian gauge theories can be asymptotically free.

Going back to eq.(33) we replace $\beta(\alpha) \sim \pm b\alpha^2$, do the integral and perform a simple algebra. We find

$$\text{QED}: \qquad \alpha(\text{t}) \sim \frac{\alpha}{1 - \text{b}\alpha\text{t}} \tag{44}$$

and

$$\text{QCD}: \qquad \alpha(\text{t}) \sim \frac{\alpha}{1 + \text{b}\alpha\text{t}} \tag{45}$$

A slightly different form is often used in QCD. Defining $1/\alpha = b \log \mu^2/\Lambda^2_{QCD}$ we can write:

$$\alpha(t) \sim \frac{1}{\frac{1}{\alpha} + bt} = \frac{1}{b \log \frac{\mu^2}{\Lambda^2_{QCD}} + b \log \frac{Q^2}{\mu^2}} = \frac{1}{b \log \frac{Q^2}{\Lambda^2_{QCD}}} \tag{46}$$

We see that $\alpha(t)$ decreases logarithmically with Q^2 and that one can introduce a dimensional parameter Λ_{QCD} that replaces μ. Often in the following we will simply write Λ for Λ_{QCD}, assuming that confusion with $\Lambda =$ ultraviolet cut-off is avoided by the reader. Note that it is clear that Λ depends on the particular definition of α, not only on the defining scale μ but also on the renormalisation scheme (see, for example, the discussion in the next session). Through the parameter b, and in general through the β function, it also depends on the number n_f of coupled flavours. It is very important to note that QED and QCD are theories with "decoupling": up to the scale Q only quarks with masses $m << Q$ contribute to the running of α. This is clearly very important, given that all applications of perturbative QCD so far apply to energies below the top quark mass m_t. For the validity of the decoupling theorem it is necessary that the theory where all the heavy particle internal lines are eliminated is still renormalisable and that the coupling constants do not vary with the mass. These requirements are true for the mass of heavy quarks in QED and QCD, but are not true in the electroweak theory where the elimination of the top would violate $SU(2)$ symmetry (because the t and b left quarks are in a doublet) and the quark couplings to the Higgs multiplet (hence to the longitudinal gauge bosons) are proportional to the mass. In conclusion, in QED and QCD, quarks with $m >> Q$ do not contribute to n_f in the coefficients of the relevant β function. The effects of heavy quarks are power suppressed and can be taken separately into account. For example, in e^+e^- annihilation for $2m_c < Q < 2m_b$ the relevant asymptotics is for $n_f = 4$, while for $2m_b < Q < 2m_t$ $n_f = 5$. Going accross the b threshold the β function coefficients change, so the $\alpha(t)$ slope changes. But $\alpha(t)$ is continuous, so that Λ changes so as to keep constant $\alpha(t)$ at the matching point at $Q \sim o(m_b)$. The effect on Λ is large: approximately $\Lambda_5 \sim 0.65\Lambda_4$.

Note the presence of a pole in eqs.(44,45) at $\pm b\alpha t = 1$, called the Landau pole, who realised its existence in QED already in the '50's. For $\mu \sim m_e$ (in QED) the pole occurs beyond the Planck mass. In QCD the Landau pole is located for negative t or at $Q < \mu$ in the region of light hadron masses. Clearly the issue of the definition and the behaviour of the physical coupling in the region around the Landau pole is a problem that lies outside the domain of perturbative QCD.

The non leading terms in the asymptotic behaviour of the running coupling can in principle be evaluated going back to eq.(41) and computing b' at 2-loops and so on. But in general the perturbative coefficients of $\beta(\alpha)$ depend on the definition of the renormalised coupling α (the renormalisation scheme), so one wonders whether it is worthwhile to do a complicated calculation to get b' if then it must be repeated for a different definition or scheme. In this respect it is

interesting to remark that actually both b and b' are independent of the definition of α, while higher order coefficients do depend on that. Here is the simple proof. Two different perturbative definitions of α are related by $\alpha' \sim \alpha(1 + c_1\alpha + ...)$. Then we have:

$$\begin{aligned} \beta(\alpha') = \frac{d\alpha'}{d\log\mu^2} &= \frac{d\alpha}{d\log\mu^2}(1 + 2c_1\alpha + ...) \\ &= \pm b\alpha^2(1 + b'\alpha + ...)(1 + 2c_1\alpha + ...) \\ &= \pm b\alpha'^2(1 + b'\alpha' + ... \end{aligned} \tag{47}$$

which shows that, up to the first subleading order, $\beta(\alpha')$ has the same form as $\beta(\alpha)$.

In QCD ($N_C = 3$) one has calculated:

$$b' = \frac{153 - 19n_f}{2\pi(33 - 2n_f)} \tag{48}$$

By taking b' into account one can write the expression of the running coupling at next to the leading order (NLO):

$$\alpha(Q^2) = \alpha_{LO}(Q^2)[1 - b'\alpha_{LO}(Q^2)\log\log\frac{Q^2}{\Lambda^2} + ...] \tag{49}$$

where $\alpha_{LO}^{-1} = b\log Q^2/\Lambda^2$ is the LO result.

Summarizing, we started from massless classical QCD which is scale invariant. But we have seen that the procedure of quantisation, regularisation and renormalisation necessarily breaks scale invariance. In the quantum QCD theory there is a scale of energy, Λ_{QCD}, which from experiment is of the order of a few hundred MeV, its precise value depending on the definition, as we shall see in detail. Adimensional quantities depend on the energy scale through the running coupling which is a logarithmic function of Q^2/Λ^2. In QCD the running coupling decreases logarithmically at large Q^2 (asymptotic freedom), while in QED the coupling has the opposite behaviour.

4 MORE ON THE RUNNING COUPLING

In the previous section we have introduced the renormalised coupling α in terms of the 3-gluon vertex at $p^2 = -\mu^2$ (momentum subtraction). The Ward identities of QCD then ensure that the coupling defined from other vertices like the $\bar{q}qg$ vertex are renormalised in the same way and the finite radiative corrections are related. But at present the universally adopted definition of α_s is in terms of dimensional regularisation because of computational simplicity which is essential given the great complexity of present day calculations. So we now briefly review the principles of dimensional regularisation and the definition of Minimal Subtraction (MS) and Modified Minimal Subtraction ($\overline{MS}$). The $\overline{MS}$ definition of α_s is the one most commonly adopted in the literature and a value quoted for it is nomally referring to this definition.

Dimensional Regularisation (DR) is a gauge and Lorentz invariant regularisation that consists in formulating the theory in $D < 4$ spacetime dimensions in order to make loop integrals ultraviolet finite. In DR one rewrites the theory in D dimensions (D is integer at the beginning, but then we will see that the expression of diagrams makes sense at all D except for isolated singularities). The metric tensor is extended into a $D \times D$ matrix $g_{\mu\nu} = diag(1, -1, -1, ..., -1)$ and 4-vectors are given by $k^\mu = (k^0, k^1, ..., k^{D-1})$. The Dirac γ^μ are $f(D) \times f(D)$ matrices and it is not important what is the precise form of the function $f(D)$. It is sufficient to extend the usual algebra in a straightforward way like $\gamma^\mu\gamma^\nu\gamma_\mu = -(D-2)\gamma^\nu$ or $Tr(\gamma^\mu\gamma^\nu) = f(D)g_{\mu\nu}$.

The physical dimensions of fields change in D dimensions and, as a consequence, the gauge couplings become dimensional $e_D = \mu^\epsilon e$, where e is adimensional, $D = 4 - 2\epsilon$ and μ is a scale

of mass (this is how a scale of mass is introduced in the DR of massless QCD!). The dimension of fields is determined by requiring that the action $S = \int d^D x \mathcal{L}$ is adimensional. By inserting for $\mathcal{L}$ terms like $m\bar{\Psi}\Psi$ or $m^2\phi^\dagger\phi$ or $e\bar{\Psi}\gamma^\mu\Psi A_\mu$ the dimensions of the fields and coupling are determined as: $m, \Psi, \phi, A_\mu, e = 1, (D-1)/2, (D-2)/2, (D-2)/2, (4-D)/2$, respectively. The formal expression of loop integrals can be written for any D. For example:

$$\int \frac{d^D k}{(2\pi)^D} \frac{1}{(k^2 - m^2)^2} = \frac{\Gamma(2 - D/2)(-m^2)^{D/2-2}}{(4\pi)^{D/2}} \tag{50}$$

For $D = 4 - 2\epsilon$ one can expand using:

$$\Gamma(\epsilon) = \frac{1}{\epsilon} - \gamma_E + o(\epsilon), \qquad \gamma_E = 0.5772..... \tag{51}$$

For some Green function G, normalised to 1 in lowest order, (like V/e with V the 3-g vertex function at the symmetric point $p^2 = q^2 = r^2$, considered in the previous section) we typically find at 1-loop:

$$G_{bare} = 1 + \alpha_0 (\frac{-\mu^2}{p^2})^\epsilon [c(\frac{1}{\epsilon} + \log 4\pi - \gamma_E) + d + o(\epsilon)] \tag{52}$$

In $\bar{M}\bar{S}$ one rewrites this at 1-loop accuracy (diagram by diagram: this is a virtue of the method):

$$\begin{aligned} G_{bare} &= Z G_{ren} \\ Z &= 1 + \alpha [c(\frac{1}{\epsilon} + \log 4\pi - \gamma_E)] \\ G_{ren} &= 1 + \alpha [c \log \frac{-\mu^2}{p^2} + d] \end{aligned} \tag{53}$$

In the original MS prescription only $1/\epsilon$ was subtracted (that clearly plays the role of a cutoff) and not also $\log 4\pi$ and γ_E. Later, since these constants always appear from the expansion of Γ functions it was decided to modify MS into $\overline{MS}$. Note that the $\overline{MS}$ definition of α is different than that in the momentum subtraction scheme because the finite terms (those beyond logs) are different. In particular here δG_{ren} does not vanish at $p^2 = -\mu^2$.

The third coefficient of the QCD β function is also known in the $\overline{MS}$ prescription (recall that only the first two coefficients are scheme independent). Translated in numbers, for $n_f = 5$ one obtains [5]:

$$\beta(\alpha) = -0.610\alpha^2[1 + 1.261...\frac{\alpha}{\pi} + 1.475...(\frac{\alpha}{\pi})^2 + ...] \tag{54}$$

It is interesting to remark that the expansion coefficients are all of order 1, so that the $\bar{M}\bar{S}$ expansion looks well behaved.

5 APPLICATION TO HARD PROCESSES

5.1 $R_{e^+e^-}$ and Related Processes

The simplest hard process is $R_{e^+e^-}$ that we have already started to discuss. R is adimensional and in perturbation theory is given by $R = N_C \sum_i Q_i^2 F(t, \alpha_s)$, where $F = 1 + o(\alpha_S)$. We have already mentioned that for this process the "anomalous dimension" function vanishes: $\gamma(\alpha_s) = 0$ because of electric charge non renormalisation by strong interactions. Let us review how this happens in detail. The diagrams that are relevant for charge renormalisation in QED at 1-loop are shown in Fig. 8. The Ward identity that follows from gauge invariance in QED imposes that

the vertex (Z_V) and the self-energy (Z_f) renormalisation factors cancel and the only divergence remains in Z_γ, the vacuum polarization of the photon. So the charge is only renormalised by the photon blob, hence it is universal (the same factor for all fermions, independent of their charge) and is not affected by QCD at 1-loop. It is true that at higher orders the photon vacuum polarization diagram is affected by QCD (for example, at 2-loops we can exchange a gluon between the quarks in the photon loop) but the renormalisation induced by the vacuum polarisation diagram remains independent of the nature of the fermion to which the photon line is attached. The gluon contributions to the vertex (Z_V) and to the self-energy (Z_f) cancel because they have exactly the same structure as in QED, and there is no gluon contribution to the lowest order photon vacuum polarisation blob. So $\gamma(\alpha_s) = 0$.

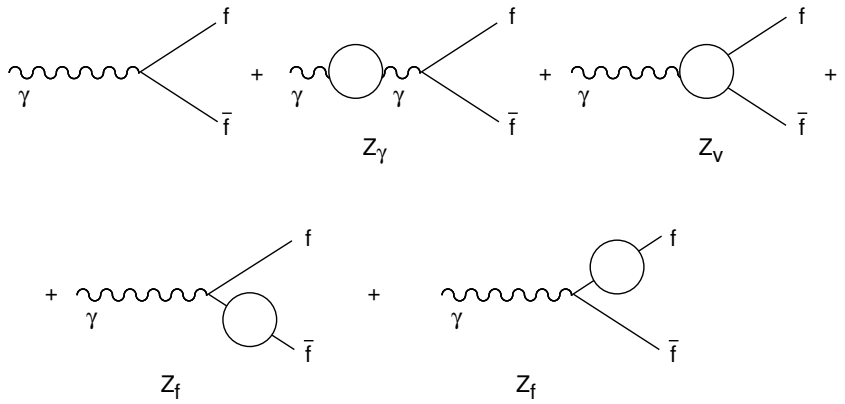

Fig. 8:

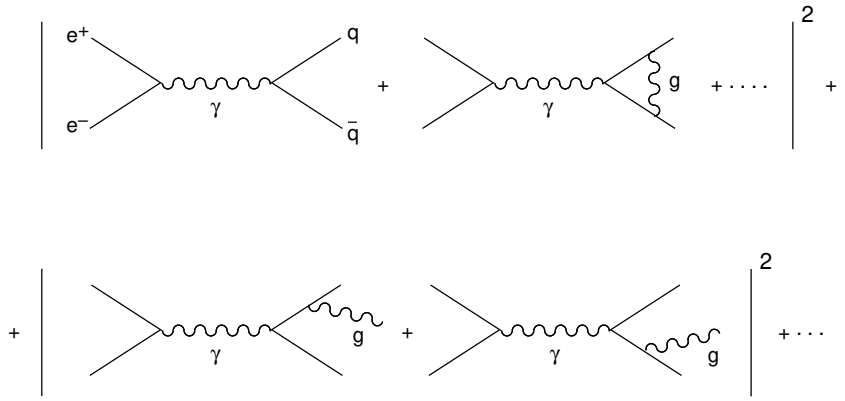

Fig. 9:

At 1-loop the diagrams relevant for the computation of R are shown in Fig. 9. There are virtual diagrams and real diagrams with one additional gluon in the final state. Infrared divergences cancel between the interference term of the virtual diagrams and the absolute square of the real diagrams, according to the Bloch-Nordsieck theorem. Similarly there are no mass singularities, in agreement with the Kinoshita-Lee-Nauenberg theorem, because the initial state is purely leptonic and all degenerate states that can appear at the given order are included in the final state. Given that $\gamma(\alpha_s) = 0$ the RGE prediction is simply given, as we have already seen, by $F(t, \alpha_s) = F[0, \alpha_s(t)]$. This means that if we do, for example, a 2-loop calculation, we

must obtain a result of the form:

$$F(t,\alpha_s) \;=\; 1 \;+\; c_1\alpha_s(1-b\alpha_s t) \;+\; c_2\alpha_s^2 \;+o(\alpha_s^3) \tag{55}$$

In fact we see that this form, taking into account that from eq.(45) we have:

$$\alpha_s(t) \;\sim\; \frac{\alpha_s}{1+b\alpha_s t} \sim \alpha_s(1 \;-\; b\alpha_s t \;+\; ....) \tag{56}$$

can be rewritten as

$$F(t,\alpha_s) \;=\; 1 \;+\; c_1\alpha_s(t) \;+\; c_2\alpha_s^2(t) \;+o(\alpha_s^3(t)) \;=\; F[0,\alpha_s(t)] \tag{57}$$

The content of the RGE prediction is, at this order, that there are no $\alpha_s t$ and $(\alpha_s t)^2$ terms (the leading log sequence must be absent) and the term of order $\alpha_s^2 t$ has the coefficient that allows to reabsorb it in the transformation of α_s into $\alpha_s(t)$.

At present the first 3 coefficients have been computed in the $\bar{M}\bar{S}$ scheme [6]. Clearly $c_1 = 1/\pi$ does not depend on the definition of α_s but c_2 and c_3 do. The subleading coefficients also depend on the scale choice: if instead of expanding in $\alpha_s(Q)$ we decide to choose $\alpha_s(Q/2)$ the coefficients c_2 and c_3 change. In the $\bar{M}\bar{S}$ scheme, for γ-exchange and $n_f = 5$, which are good approximations for $2m_b << Q << m_Z$, one has:

$$F[0,\alpha_s(t)] \;=\; 1 \;+\; \frac{\alpha_s(t)}{\pi} \;+\; 1.409...(\frac{\alpha_s(t)}{\pi})^2 \;-\; 12.8...(\frac{\alpha_s(t)}{\pi})^3 \;+...\tag{58}$$

Similar perturbative results at 3-loop accuracy also exist for $R_Z = \Gamma(Z \to hadrons)/\Gamma(Z \to leptons)$, $R_\tau = \Gamma(\tau \to \nu_\tau + hadrons)/\Gamma(\tau \to \nu_\tau + leptons)$, etc. We will discuss these results later when we deal with measurements of α_s.

The perturbative expansion in powers of $\alpha_s(t)$ takes into account all contributions that are suppressed by powers of logarithms of the large scale Q^2 ("leading twist" terms). In addition there are corrections suppressed by powers of the large scale Q^2 ("higher twist" terms). The pattern of power corrections is controlled by the light-cone Operator Product Expansion (OPE) which (schematically) leads to:

$$F \;=\; \text{pert.} \;+\; \mathrm{r}_2\frac{\mathrm{m}^2}{\mathrm{Q}^2} \;+\; \mathrm{r}_4\frac{<0|\mathrm{Tr}[\mathbf{F}_{\mu\nu}\mathbf{F}^{\mu\nu}]|\mathbf{0}>}{\mathrm{Q}^4} \;+\; ... \;+\; \mathrm{r}_6\frac{<0|\mathrm{O}_6|0>}{\mathrm{Q}^6} \;+\; ... \tag{59}$$

Here m^2 generically indicates mass corrections, notably from b quarks, for example (t quark mass corrections only arise from loops, vanish in the limit $m_t \to \infty$ and are included in the coefficients as those in eq.(58) and the analogous ones for higher twist terms), $\mathbf{F}_{\mu\nu} = \sum_{\mathbf{A}} \mathbf{F}^{\mathbf{A}}_{\mu\nu}\mathbf{t}^{\mathbf{A}}$, O_6 is typically a 4-fermion operator, etc. For each possible gauge invariant operator the corresponding power of Q^2 is fixed by dimensions.

We now consider the light-cone OPE in some more detail. $R_{e^+e^-} \sim \Pi(Q^2)$ where $\Pi(Q^2)$ is the scalar spectral function related to the hadronic contribution to the imaginary part of the photon vacuum polarization $T_{\mu\nu}$:

$$\begin{aligned} T_{\mu\nu} \;&=\; (-g_{\mu\nu}Q^2 \;+\; q_\mu q_\nu)\Pi(Q^2) \;=\; \int \exp iqx <0|J_\mu^\dagger(x)J_\nu(0)|0> dx \;= \\ &=\; \sum_n <0|J_\mu^\dagger(0)|n><n|J_\nu(0)|0> (2\pi)^4\delta^4(q-p_n) \end{aligned} \tag{60}$$

For $Q^2 \to \infty$ the $x^2 \to 0$ region is dominant. To all orders in perturbation theory the OPE can be proven. Schematically, dropping Lorentz indices, for simplicity, near $x^2 \sim 0$ we have:

$$J^\dagger_\mu(x)J_\nu(0) \;=\; I(x^2) \;+\; E(x^2)\sum_{n=0}^{\infty} c_n(x^2)x^{\mu_1}...x^{\mu_n}\cdot O^n_{\mu_1...\mu_n}(0) \;+ \\ +\; \text{less sing. terms} \tag{61}$$

Here $I(x^2)$, $E(x^2)$,..., $c_n(x^2)$ are c-number singular functions, O^n is a string of local operators. $E(x^2)$ is the singularity of free field theory, $I(x^2)$ and $c_n(x^2)$ contain powers of $\log \mu x$ in interaction. Some O^n are already present in free field theory, other ones appear when interactions are switched on. $\Pi(Q^2)$ is related to the Fourier transform. Less singular terms in x^2 lead to power suppressed terms in $1/Q^2$. The perturbative terms come from $I(x^2)$ which is the leading twist term. The logarithmic scaling violations induced by the running coupling are the logs in $I(x^2)$.

5.2 The Final State in e^+e^- Annihilation

Experiments on e^+e^- annihilation at high energy provide a remarkable possibility of systematically testing the distinct signatures predicted by QCD for the structure of the final state averaged over a large number of events. Typical of asymptotic freedom is the hierarchy of configurations emerging as a consequence of the smallness of $\alpha_s(Q^2)$. When all corrections of order $\alpha_s(Q^2)$ are neglected one recovers the naive parton model prediction for the final state: almost collinear events with two back-to-back jets with limited transverse momentum and an angular distribution as $(1+\cos^2\theta)$ with respect to the beam axis (typical of spin 1/2 parton quarks: scalar quarks would lead to a $\sin^2\theta$ distribution). At order $\alpha_s(Q^2)$ a tail of events is predicted to appear with large transverse momentum $p_T \sim Q/2$ with respect to the thrust axis (the axis that maximizes the sum of the absolute values of the longitudinal momenta of the final state particles). This small fraction of events with large p_T mostly consists of three-jet events with an almost planar topology. The skeleton of a three-jet event, at leading order in $\alpha_s(Q^2)$, is formed by three hard partons $q\bar{q}g$, the third being a gluon emitted by a quark or antiquark line. The distribution of three-jet events is given by:

$$\frac{1}{\sigma}\frac{d\sigma}{dx_1 dx_2} \;=\; \frac{2\alpha_s}{3\pi}\frac{x_1^2+x_2^2}{(1-x_1)(1-x_2)} \tag{62}$$

here $x_{1,2}$ refer to energy fractions of massless quarks: $x_i = 2E_i/\sqrt{s}$ with $x_1+x_2+x_3=2$. At order $\alpha_s^2(Q^2)$ a hard perturbative non planar component starts to build up and a small fraction of four-jet events $q\bar{q}gg$ or $q\bar{q}q\bar{q}$ appear, and so on.

For precise testing and for measuring α_s a quantitatively specified definition of jet counting must be introduced which must be infrared safe (i.e. not altered by soft particle emission or collinear splittings of massless particles) in order to be computable at parton level and as much as possible insensitive to the transformation of partons into hadrons. One introduces a resolution parameter y_{cut} and a suitable pair variable, for example:

$$y_{ij} \;=\; \frac{min(E_i^2, E_j^2)(1-\cos\theta_{ij})}{s} \tag{63}$$

The particles i,j belong to different jets for $y_{ij} > y_{cut}$. Clearly the number of jets becomes a function of y_{cut}: there are more jets for smaller y_{cut}. Measurements of $\alpha_s(Q^2)$ have been performed starting from jet multiplicities, the largest error coming from the necessity of correcting for non-perturbative hadronisation effects.

5.3 Deep Inelastic Scattering

Deep Inelastic Scattering (DIS) processes have played and still play a very important role for our understanding of QCD and of nucleon structure. This set of processes actually provides us with a rich laboratory for theory and experiment. There are several structure functions that can be studied, $F_i(x, Q^2)$, each a function of two variables. This is true separately for different beams and targets and different polarizations. Depending on the charges of l and l' we can have neutral currents (γ,Z) or charged currents in the l'-l channel (Fig. 6). In the past DIS processes were crucial for establishing quarks and gluons as partons and QCD as the theory of strong interactions. At present DIS is very important for quantitative studies and tests of QCD. The theory of scaling violations for totally inclusive DIS structure functions, based on operator expansions and renormalization group techniques, is crystal clear and the predicted Q^2 dependence can be tested at each value of x. The measurement of quark and gluon densities in the nucleon, as functions of x at some reference value of Q^2, which is an essential starting point for the calculation of all relevant hadronic hard processes, is performed in DIS processes. At the same time one measures $\alpha_s(Q^2)$ and the DIS values can be compared with those obtained from other processes. At all times new theoretical challenges arise from the study of DIS processes. Recent examples are the so-called "spin crisis" in polarized DIS and the behaviour of singlet structure functions at small x as revealed by HERA data. In the following we will review the past successes and the present open problems in the physics of DIS.

The cross-section $\sigma \sim L^{\mu\nu} W_{\mu\nu}$ is given in terms of the product of a leptonic ($L^{\mu\nu}$) and a hadronic ($W_{\mu\nu}$) tensor. While $L^{\mu\nu}$ is simple and easily obtained from the lowest order electroweak (e-w) vertex plus QED radiative corrections, the complicated strong interaction dynamics is contained in $W_{\mu\nu}$. The latter is proportional to the Fourier transform of the forward matrix element between the nucleon target states of the product of two e-w currents:

$$W_{\mu\nu} \;=\; \int dx \;\; \exp iqx \;\; < p|J^{\dagger}_{\mu}(x) J_{\nu}(0)|p > \tag{64}$$

Structure functions are defined starting from the general form of $W_{\mu\nu}$ given Lorentz invariance and current conservation. For example, for e-w currents between unpolarized nucleons we have:

$$\begin{aligned} W_{\mu\nu} \;\; = \;\; & (-g_{\mu\nu} \;+\; \frac{q_\mu q_\nu}{q^2})\; W_1(\nu, Q^2) \;+\; (p_\mu \;-\; \frac{m\nu}{q^2} q_\mu)(p_\nu \;-\; \frac{m\nu}{q^2} q_\nu)\; \frac{W_2(\nu, Q^2)}{m^2} \;- \\ & - \;\; \frac{i}{2m^2} \epsilon_{\mu\nu\lambda\rho} p^\lambda q^\rho \;\; W_3(\nu, Q^2) \end{aligned}$$

W_3 is absent for pure vector currents. In the limit $Q^2 >> m^2$, x fixed, the structure functions obey approximate Bjorken scaling which in reality is broken by logarithmic corrections that can be computed in QCD:

$$\begin{aligned} m W_1(\nu, Q^2) &\to F_1(x) \\ \nu W_{2,3}(\nu, Q^2) &\to F_{2,3}(x) \end{aligned} \tag{65}$$

The $\gamma - N$ cross-section is given by ($W_i \;=\; W_i(Q^2, \nu)$):

$$\frac{d\sigma^\gamma}{dQ^2 d\nu} \;=\; \frac{4\pi\alpha^2 E'}{Q^4 E} \cdot [2\sin^2\theta/2 W_1 \;+\; \cos^2\theta/2 W_2] \tag{66}$$

while for the $\nu - N$ or $\bar{\nu} - N$ cross-section one has:

$$\frac{d\sigma^{\nu,\bar{\nu}}}{dQ^2 d\nu} \;=\; \frac{G_F^2 E'}{2\pi E} (\frac{m_W^2}{Q^2 + m_W^2})^2 \cdot [2\sin^2\theta/2 W_1 \;+\; \cos^2\theta/2 W_2 \pm \frac{E + E'}{m} \sin^2\theta/2 W_3] \tag{67}$$

(W_i for photons, ν and $\bar{\nu}$ are all different, as we shall see in a moment).

In the scaling limit the longitudinal and transverse cross sections are given by:

$$\begin{aligned} \sigma_L &= \frac{1}{s}[\frac{F_2(x)}{2x} - F_1(x)] \\ \sigma_{RH,LH} &\sim \frac{1}{s}[F_1(x) \pm F_3(x)] \\ \sigma_T &= \sigma_{RH} + \sigma_{LH} \end{aligned} \tag{68}$$

where L, RH, LH refer to the helicity 0, 1, -1, respectively, of the exchanged gauge vector boson.

In the '60's the demise of hadrons from the status of fundamental particles to that of bound states of constituent quarks was the breakthrough that made possible the construction of a renormalisable field theory for strong interactions. The presence of an unlimited number of hadrons species, many of them with large spin values, presented an obvious dead-end for a manageable field theory. The evidence for constituent quarks emerged clearly from the systematics of hadron spectroscopy. The complications of the hadron spectrum could be explained in terms of the quantum numbers of spin 1/2, fractionally charged, u, d and s quarks. The notion of colour was introduced to reconcile the observed spectrum with Fermi statistics. But confinement that forbids the observation of free quarks was a clear obstacle towards the acceptance of quarks as real constituents and not just as fictitious entities describing some mathematical pattern (a doubt expressed even by Gell-Mann at the time). The early measurements at SLAC of DIS dissipated all doubts: the observation of Bjorken scaling and the success of the naive (not so much after all) parton model of Feynman imposed quarks as the basic fields for describing the nucleon structure (parton quarks).

In the language of Bjorken and Feynman the virtual γ (or, in general, any gauge boson) sees the quark partons inside the nucleon target as quasi-free, because the (Lorentz dilated) QCD interaction time is much longer than $\tau_\gamma \sim 1/Q$. Since the virtual photon 4-momentum is spacelike, we can go to a Lorentz frame where $E_\gamma = 0$ (Breit frame). In this frame $q = (E_\gamma = 0; 0, 0, Q)$ and the nucleon momentum, neglecting the mass $m << Q$, is $p = (Q/2x; 0, 0, -Q/2x)$ (note that this correctly gives $x = Q^2/2(p \cdot q)$). Consider (Fig. 10) the interaction of the photon with a quark carrying a fraction y of the nucleon 4-momentum: $p_q = yp$ (we are neglecting the transverse components of p_q which are of order m). The incoming parton with $p_q = yp$ absorbs the photon and the final parton has 4-momentum p'_q. Since in the Breit frame the photon carries no energy but only a longitudinal momentum Q, the photon can only be absorbed by those partons with $y = x$: then the longitudinal component of $p_q = yp$ is $-yQ/2x = -Q/2$ and can be flipped into $+Q/2$ by the photon. As a result, the photon longitudinal momentum $+Q$ disappears, the parton quark momentum changes of sign from $-Q/2$ into $+Q/2$ and the energy is not changed. So the structure functions are proportional to the density of partons with fraction x of the nucleon momentum, weighted with the squared charge. Also, recall that the helicity of a massless quark is conserved in a vector (or axial vector) interaction. So when the momentum is reversed also the spin must flip. Since the process is collinear there is no orbital contribution and only a photon with helicity ± 1 (transverse photon) can be absorbed. If partons were spin zero only longitudinal photons would instead contribute.

Using these results, which are maintained in QCD at leading order, the quantum numbers of the quarks were confirmed by early experiments. The observation that $R = \sigma_L/\sigma_T \to 0$ implies that the charged partons have spin 1/2. The quark charges were derived from the data on the electron and neutrino structure functions:

$$\begin{aligned} F_{ep} &= 4/9u(x) + 1/9d(x) + ...; \qquad F_{en} = 4/9d(x) + 1/9u(x) + ... \\ F_{\nu p} &= F_{\bar{\nu} n} = 2d(x) + ...; \qquad F_{\nu n} = F_{\bar{\nu} p} = 2u(x) + ... \end{aligned} \tag{69}$$

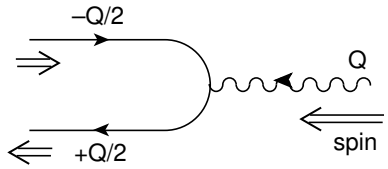

Fig. 10:

where $F \sim 2F_1 \sim F_2/x$ and $u(x)$, $d(x)$ are the parton number densities in the proton (with fraction x of the proton longitudinal momentum), which, in the scaling limit, do not depend on Q^2. The normalisation of the structure functions and the parton densities are such that the charge relations hold:

$$\int_0^1 [u(x) - \bar{u}(x)]dx = 2, \quad \int_0^1 [d(x) - \bar{d}(x)]dx = 1, \quad \int_0^1 [s(x) - \bar{s}(x)]dx = 0 \tag{70}$$

Also it was proven by experiment that at values of Q^2 of a few GeV^2, in the scaling region, about half of the nucleon momentum, given by the momentum sum rule:

$$\int_0^1 [\sum_i (q_i(x) + \bar{q}_i(x)) \ + \ g(x)]xdx \ = \ 1 \tag{71}$$

is carried by neutral partons (gluons).

In QCD there are calculable log scaling violations induced by $\alpha_s(t)$. The parton rules just introduced can be summarised in the formula:

$$F(x,t) \ = \ \int_x^1 dy \frac{q_0(y)}{y} \sigma_{point}(\frac{x}{y}, \alpha_s(t)) \ + \ o(\frac{1}{Q^2}) \tag{72}$$

Before QCD corrections $\sigma_{point} = e^2\delta(x/y - 1)$ and $F = e^2 q_0(x)$ (here we denote by e the charge of the quark in units of the positron charge, i.e. $e = 2/3$ for the u quark). QCD modifies σ_{point} at order α_s via the diagrams of Fig. 11. Note that the integral is from x to 1, because the energy can only be lost by radiation before interacting with the photon (which eventually wants to find a fraction x, as we have explained). From a direct computation of the diagrams one obtains a result of the following form:

$$\sigma_{point}(z, \alpha_s(t)) \ \simeq \ e^2[\delta(z-1) \ + \ \frac{\alpha_s}{2\pi}(t \cdot P(z) \ + \ f(z))] \tag{73}$$

For $y > x$ the correction arises from diagrams with real gluon emission. Only the sum of the two real diagrams in Fig. 11 is gauge invariant, so that the contribution of one given diagram is gauge dependent. There is a special form of axial gauge, called physical gauge, where, among real diagrams, the diagram of Fig. 11(c) gives the whole t-proportional term. It is obviously not essential to go to this gauge, but this diagram has a direct physical interpretation: a quark in the proton has a fraction $y > x$ of the parent 4-momentum; it then radiates a gluon and looses energy down to a fraction x before interacting with the photon. The log arises from the virtual quark propagator, according to the discussion of collinear mass singularities in eq.(17). In fact in the massless limit one has:

$$\begin{aligned} \text{propagator} \quad &= \quad \frac{1}{r^2} \ = \ \frac{1}{(k-h)^2} \ = \ \frac{-1}{2E_k E_h} \cdot \frac{1}{1-\cos\theta} \\ &= \ \frac{-1}{4E_k E_h} \cdot \frac{1}{\sin^2\theta/2} \ \propto \frac{-1}{p_T^2} \end{aligned} \tag{74}$$

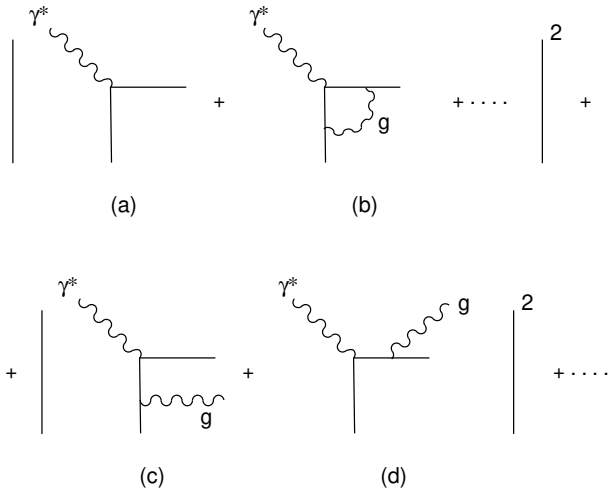

Fig. 11:

where p_T is the transverse momentum of the virtual quark. So the square of the propagator goes like $1/p_T^4$. But there is a p_T^2 factor in the numerator, because in the collinear limit, when $\theta = 0$ and the initial and final quarks and the emitted gluon are all aligned, the quark helicity cannot flip (vector interaction) and the real gluon cannot have but ± 1 helicity. So the cross-section behaves as:

$$\sigma \sim \int^{Q^2} \frac{1}{p_T^2} dp_T^2 \sim \log Q^2 \tag{75}$$

Actually the log should be read as $\log Q^2/m^2$ because in the massless limit a genuine mass singularity appears. In fact the mass singularity connected with the initial quark line is not cancelled because we do not have the sum of all degenerate initial states, but only a single quark. But in correspondence to the initial quark we have the (bare) quark density $q_0(y)$ that appear in the convolution integral. This is a non perturbative quantity that is determined by the nucleon wave function. So we can factorize the mass singularity in a redefinition of the quark density: we replace $q_0(y) \to q(y,t) = q_0(y) + \Delta q(y,t)$ with:

$$\Delta q(y,t) = \frac{\alpha_s}{2\pi} t \int_x^1 dy \frac{q_0(y)}{y} \cdot P(\frac{x}{y}) \tag{76}$$

Here the factor of t is a bit symbolic: it stands for $\log Q^2/km^2$ and what we exactly put below Q^2 depends on the definition of the renormalised quark density, that also determines the exact form of the finite term $f(z)$ in eq.(73).

The effective parton density $q(y,t)$ that we have defined is now scale dependent. In terms of this scale dependent density we have the following relations, where we have also replaced the fixed coupling with the running coupling according to the prescription derived from the RGE:

$$\begin{aligned} F(x,t) &= \int_x^1 dy \frac{q(y,t)}{y} e^2 [\delta(\frac{x}{y} - 1) + \frac{\alpha_s(t)}{2\pi} f(\frac{x}{y}))] = e^2 q(x,t) + o(\alpha_s(t)) \\ \frac{d}{dt} q(x,t) &= \frac{\alpha_s(t)}{2\pi} \int_x^1 dy \frac{q(y,t)}{y} \cdot P(\frac{x}{y}) + o(\alpha_s(t)^2) \end{aligned} \tag{77}$$

We see that in lowest order we reproduce the naive parton model formulae for the structure functions in terms of effective parton densities that are scale dependent. The evolution equations

for the parton densities are written down in terms of kernels (the "splitting functions") that can be expanded in powers of the running coupling. At leading order, we can interpret the evolution equation by saying that the variation of the quark density at x is given by the convolution of the quark density at y times the probability of emitting a gluon with fraction x/y of the quark momentum.

It is interesting that the integro-differential QCD evolution equation for densities can be transformed into an ordinary differential equation for Mellin moments. The moment f_n of a density $f(x)$ is defined as:

$$f_n \;=\; \int_0^1 dx x^{n-1} f(x) \tag{78}$$

By taking moments of both sides of the second of eqs.(77) one finds, with a simple interchange of the integration order, the simpler equation for the nth moment:

$$\frac{d}{dt} q_n(t) \;=\; \frac{\alpha_s(t)}{2\pi} \cdot P_n \cdot q_n(t) \tag{79}$$

To solve this equation we observe that:

$$\log \frac{q_n(t)}{q_n(0)} \;=\; \frac{P_n}{2\pi} \int_0^t \alpha_s(t) dt \;=\; \frac{P_n}{2\pi} \int_{\alpha_s}^{\alpha_s(t)} \frac{d\alpha'}{-b\alpha'} \tag{80}$$

where we used eq.(36) to change the integration variable from dt to $d\alpha(t)$ (denoted as $d\alpha'$) and $\beta(\alpha) \simeq -b\alpha^2 + ...$ Finally the solution is:

$$q_n(t) \;=\; [\frac{\alpha_s}{\alpha_s(t)}]^{\frac{P_n}{2\pi b}} \cdot q_n(0) \tag{81}$$

The connection of these results with the RGE general formalism occurs via the light cone OPE (recall eq.(64) for $W_{\mu\nu}$ and eq.(61) for the OPE of two currents). In the case of DIS the c-number term $I(x^2)$ does not contribute, because we are interested in the connected part $< p|...|p > - < 0|...|0 >$. The relevant terms are:

$$J^\dagger_\mu(x) J_\nu(0) \;=\; E(x^2) \sum_{n=0}^{\infty} c_n(x^2) x^{\mu_1} ... x^{\mu_n} \cdot O^n_{\mu_1 ... \mu_n}(0) \;+\; \text{less sing. terms} \tag{82}$$

A formally intricate but conceptually simple argument (Ref.[3], page 28) based on the analiticity properties of the forward virtual Compton amplitude shows that the Mellin moments M_n of structure functions are related to the individual terms in the OPE, precisely to the Fourier transform $c_n(Q^2)$ (we will write it as $c_n(t, \alpha)$) of the coefficient $c_n(x^2)$ times a reduced matrix element h_n from the operators O^n: $< p|O^n_{\mu_1 ... \mu_n}(0)|p >= h_n p_{\mu_1} ... p_{\mu_n}$:

$$c_n < p|O^n|p > \to M_n = \int_0^1 dx x^{n-1} F(x) \tag{83}$$

Since the matrix element of the products of currents satisfy the RGE so do the moments M_n. Hence the general form of the Q^2 dependence is given by the RGE solution (see eq.(38)):

$$M_n(t, \alpha) \;=\; c_n[0, \alpha(t)] \exp \int_\alpha^{\alpha(t)} \frac{\gamma_n(\alpha')}{\beta(\alpha')} d\alpha' \cdot h_n(\alpha) \tag{84}$$

In lowest order, identifying in the simplest case M_n with q_n, we have:

$$\gamma_n(\alpha) \;=\; \frac{P_n}{2\pi}\alpha \;+\; ..., \qquad\qquad \beta(\alpha) \;=\; -\,b\alpha^2 \;+\; ... \tag{85}$$

and

$$q_n(t) = q_n(0) \exp \int_\alpha^{\alpha(t)} \frac{\gamma_n(\alpha')}{\beta(\alpha')} d\alpha' \;=\; [\frac{\alpha_s}{\alpha_s(t)}]^{\frac{P_n}{2\pi b}} \cdot q_n(0) \tag{86}$$

which exactly coincides with eq.(81).

Up to this point we have implicitely restricted our attention to non-singlet (under the flavour group) structure functions. The Q^2 evolution equations become non diagonal as soon as we take into account the presence of gluons in the target. In fact the quark which is seen by the photon can be generated by a gluon in the target (Fig. 12).

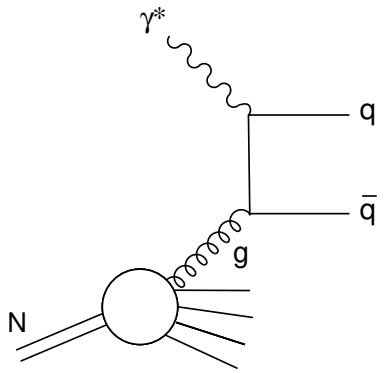

Fig. 12:

The quark evolution equation becomes:

$$\frac{d}{dt} q_i(x,t) \;=\; \frac{\alpha_s(t)}{2\pi} [q_i \bigotimes P_{qq}] \;+\; \frac{\alpha_s(t)}{2\pi} [g \bigotimes P_{qg}] \tag{87}$$

where we introduced the shorthand notation:

$$[q \bigotimes P] \;=\; [P \bigotimes q] \;=\; \int_x^1 dy \frac{q(y,t)}{y} \cdot P(\frac{x}{y}) \tag{88}$$

(it is easy to check that the convolution, like an ordinary product, is commutative). At leading order, the interpretation of eq.(87) is simply that the variation of the quark density is due to the convolution of the quark density at a higher energy times the probability of finding a quark in a quark (with the right energy fraction) plus the gluon density at a higher energy times the probability of finding a quark (of the given flavour i) in a gluon. The evolution equation for the gluon density, needed to close the system, can be obtained by suitably extending the same line of reasoning to a gedanken probe sensitive to colour charges, for example a virtual gluon. The resulting equation is of the form:

$$\frac{d}{dt} g(x,t) \;=\; \frac{\alpha_s(t)}{2\pi} [\sum_i (q_i + \bar{q}_i) \bigotimes P_{gq}] \;+\; \frac{\alpha_s(t)}{2\pi} [g \bigotimes P_{gg}] \tag{89}$$

The explicit form of the splitting functions in lowest order can be explicitly derived from the QCD vertices. They are a property of the theory and do not depend on the particular process the parton density is taking part into. The results are:

$$P_{qq} \;=\; \frac{4}{3} [\frac{1+x^2}{(1-x)_+} \;+\; \frac{3}{2} \delta(1-x)] \;+\; o(\alpha_s)$$

$$P_{gq} \;=\; \frac{4}{3} \frac{1+(1-x)^2}{x} \;+\; o(\alpha_s)$$

$$P_{qg} \;=\; \frac{1}{2}[x^2+(1-x)^2] \;+\; o(\alpha_s)$$

$$P_{gg} \;=\; 6[\frac{x}{(1-x)_+} \;+\; \frac{1-x}{x} \;+\; x(1-x)] \;+\; \frac{33-2n_f}{6}\delta(1-x) \;+\; o(\alpha_s) \qquad (90)$$

The "+" distribution is defined as, for a generic non singular weight function $f(x)$:

$$\int_0^1 \frac{f(x)}{(1-x)_+}dx \;=\; \int_0^1 \frac{f(x)-f(1)}{1-x}dx \qquad (91)$$

The $\delta(1-x)$ terms arise from the virtual corrections to the tree diagram. Their coefficient can be simply obtained by imposing the validity of charge and momentum sum rules. In fact, from the request that the charge sum rules in eq.(70) are not affected by the Q^2 dependence one derives that

$$\int_0^1 P_{qq}(x)dx \;=\; 0 \qquad (92)$$

which can be used to fix the coefficient of the $\delta(1-x)$ terms of P_{qq}. Similarly, by taking the t-derivative of the momentum sum rule in eq.(71) and imposing its vanishing for generic q_i and g, one obtains:

$$\int_0^1 [P_{qq}(x) \;+\; P_{gq}(x)]xdx \;=\; 0, \qquad \int_0^1 [2n_f P_{qg}(x) \;+\; P_{gg}(x)]xdx \;=\; 0, \qquad (93)$$

At higher orders the evolution equations are easily generalised but the calculation of the splitting functions rapidly becomes very complicated. The splitting functions are completely known at NLO accuracy: $\alpha_s P \;\sim\; \alpha_s P_1 \;+\; \alpha_s^2 P_2 \;+ ....$ More recently the NNLO results P_3 have been derived in analytic form for the first few moments [7]. The full NNLO calculation is in progress and could be finished soon.

The scaling violations are clearly observed by experiment and their pattern is very well reproduced by QCD fits at NLO. Examples are seen in Figs. 13(a-d) [8]. These fits provide an impressive confirmation of a quantitative QCD prediction, a measurement of $q_i(x,Q_0^2)$ and $g(x,Q_0^2)$ at some reference value Q_0^2 of Q^2 and a precise measurement of $\alpha_s(m_Z^2)$. At small x and large but fixed Q^2 when terms of order $(\alpha_s \log 1/x)^n$ become of order 1 and cannot be neglected, the validity of the NLO or NNLO approximations should breakdown. However, the small x data collected by HERA can be fitted reasonably even at the smallest measured values of x by the NLO QCD evolution equations, so that there is no neat evidence in the data for departures. But the extracted gluon density (which is dominant at small x) and the fitted value of $\alpha_s(m_Z^2)$ could be biassed by this effect if data at too small values of x are included.

5.4 Factorisation and the QCD Improved Parton Model

The parton densities defined and measured in DIS are used to compute hard processes initiated by hadronic collisions via the Factorisation Theorem (FT). Suppose you have a hadronic process of the form $h_1 + h_2 \to X + all$ where X is some triggering particle or pair of particles which specify the large scale Q^2 relevant for the process, in general somewhat but not much smaller than s, the total c.o.m. squared mass. For example, in pp or $p\bar{p}$ collisions, X can be a W or a Z or a virtual photon with large Q^2, or a jet at large transverse momentum p_T, or a pair of heavy quark-antiquark of mass M. By "all" we mean a totally inclusive collection of gluons and light quark pairs. The FT implies that for the cross-section or some other sufficiently inclusive distribution we can write the expression:

$$\sigma(s,\tau) \;=\; \sum_{AB} \int dx_1 dx_2 p_{1A}(x_1,Q^2) p_{2B}(x_2,Q^2) \sigma_{AB}(x_1 x_2 s,\tau) \qquad (94)$$

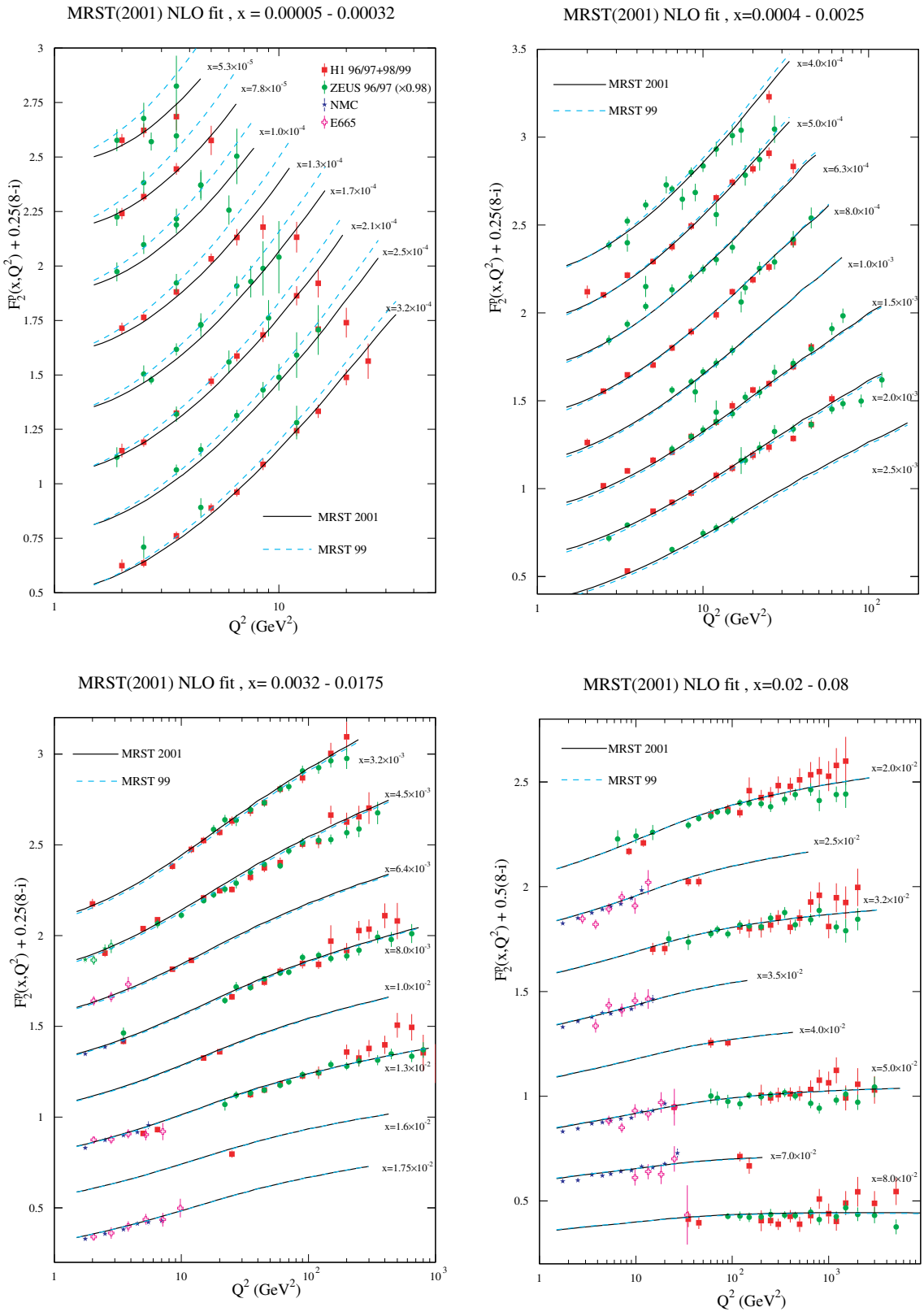

Fig. 13: A recent NLO fit of scaling violations from Ref. [8], for different x ranges, as functions of Q^2

Here $\tau = Q^2/s$ is a scaling variable, p_{iC} are generic parton-C densities inside the hadron h_i, σ_{AB} is the partonic cross-section for parton-A + parton-B$\rightarrow X + all'$. This result is based on the fact that the mass singularities that are associated with the initial legs are of universal nature, so that one can reproduce the same modified parton densities, by absorbing these singularities into the bare parton densities, as in deep inelastic scattering. Once the parton densities and α_s are known from other measurements the prediction of the rate for a given hard process is obtained with no free parameters. The NLO calculation of the reduced partonic cross-section is needed in order to correctly specify the scale and in general the definition of the parton densities and of the running coupling in the leading term. The residual scale and scheme dependence is often the most important source of theoretical error. In the following we consider a few examples.

A comparison of data and predictions on the production of jets at large $\sqrt{s}$ and p_T in pp or $p\bar{p}$ collisions is shown in Fig. 14 [4].

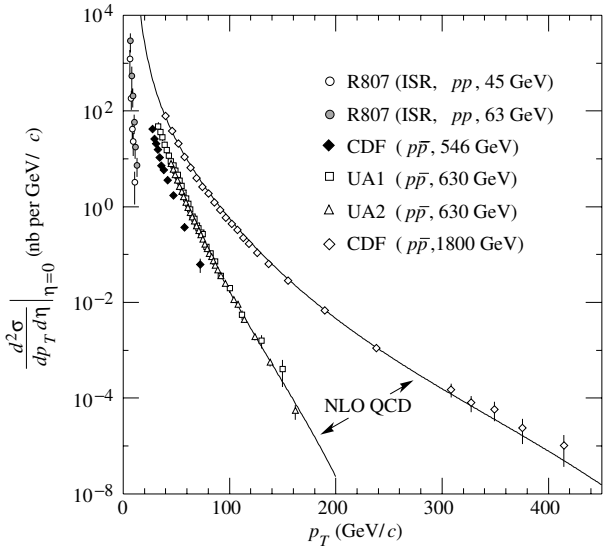

Fig. 14: Jet production cross-section at pp or $p\bar{p}$ colliders, as function of p_T

This is a particularly significant test because the rates at different c.o.m. energies and, for each energy, at different values of p_T span over many orders of magnitude. Also the corresponding values of $\sqrt{s}$ and p_T are large enough to be well inside the perturbative region. The overall agreement of the data from ISR, UA1,2 and CDF and D0 is spectacular. Only at very large p_T there might be some problem according to CDF and, to a lesser extent, to D0. A harder gluon at large x and inclusion of systematic errors can alleviate or eliminate the problem. This issue will be clarified in the near future by the RunII results at the Tevatron. Similar results also hold for the production of photons at large p_T. The collider data, shown in Fig. 15 [4], are in fair agreement with the theoretical predictions. A less clear situation is found with fixed target data. Here, first of all, the experimental results show some internal discrepancies. Also, the p_T accessible values being smaller, the theoretical uncertainties are larger. But it is true that the agreement is poor, so that the necessity of an "intrinsic" transverse momentum of partons inside the hadron of over 1 GeV has been claimed, which I do not think one is free to introduce.

For heavy quark production at colliders the agreement is very good for top production at the Tevatron (Fig. 16). To present a rare example of a puzzle, the bottom production at the Tevatron remains problematic. The total rate and the p_T distribution of b quarks observed at CDF is in excess of the prediction, up to the largest measured values of p_T (fig.17). It is true that this is a complicated case, with different scales being present at the same time: $\sqrt{s}$, p_T, m_b. Also

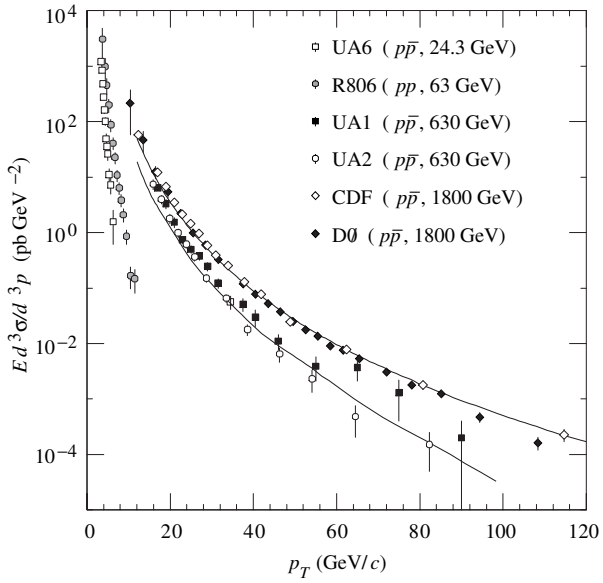

Fig. 15: Single photon production in $p\bar{p}$ colliders as function of p_T

some non-perturbative ingredients, like fragmentation functions, are present in the calculation and could be in part reponsible for the effect. But no clear explanation of this phenomenon is available. Probably it occurs through an unfavourable conspiracy of several small effects.

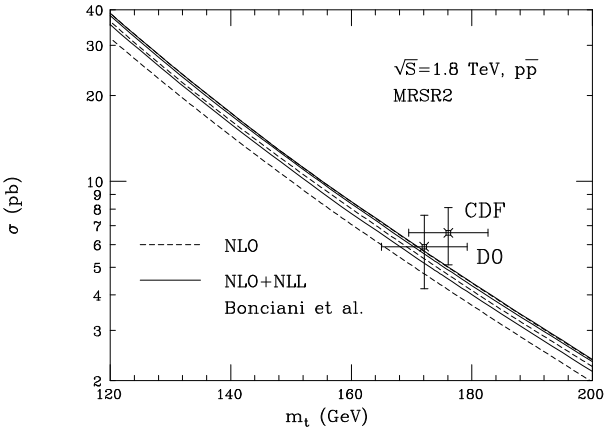

Fig. 16: The t production cross-section at the Tevatron $p\bar{p}$ collider

Drell-Yan processes, including lepton pair production via virtual γ, W or Z exchange, offer a good opportunity to test QCD. The process is quadratic in parton densities, and the final state is totally inclusive, while the large scale is specified and measured by the invariant mass squared Q^2 of the lepton pair which itself is not strongly interacting. The QCD improved parton model leads directly to a prediction for the total rate as a function of Q^2. The value of the LO cross-section is inversely proportional to the number of colours N_C because a quark of given colour can only annihilate with an antiquark of the same colour to produce a colourless lepton pair. The order $\alpha_s(Q^2)$ corrections to the total rate were computed long ago and found to be particularly large, when the quark densities are defined from the structure function F_2 measured in DIS at $q^2 = -Q^2$. The ratio $\sigma_{corr}/\sigma_{LO}$ of the corrected and the Born cross-sections,

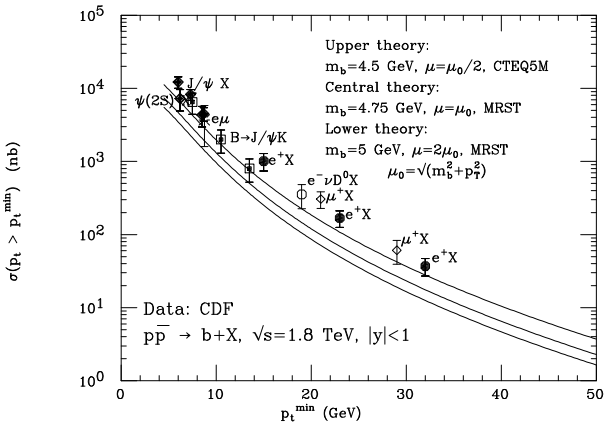

Fig. 17: The b production p_T distribution at the Tevatron $p\bar{p}$ collider (CDF collaboration). The cross-section for $p_T > p_T^{min}$ is plotted as function of p_T^{min}.

was called K-factor (by me), because it is almost a constant in rapidity. More recently also the NLO full calculation of the K-factor was completed, a very remarkable calculation [9]. The QCD predictions can be best tested for W and Z production at CERN and Tevatron energies. $Q \sim m_{W,Z}$ is large enough to make the prediction reliable (a not too large K-factor) and the ratio $\sqrt{\tau} = Q/\sqrt{s}$ is not too small. Recall that in lowest order $x_1 x_2 s = Q^2$ so that the parton densities are probed at x values around $\sqrt{\tau}$. We have $\sqrt{\tau} = 0.13 - 0.15$ at $\sqrt{s} = 630$ GeV (CERN $Sp\bar{p}S$ Collider) and $\sqrt{\tau} = 0.041 - 0.052$ at the Tevatron. In this respect the prediction is more delicate at the LHC, where $\sqrt{\tau} \sim 5.9 - 6.5 \cdot 10^{-3}$. One comparison of the experimental total rates at the Tevatron with the QCD predictions is shown in Fig. 18, together with the expected rates at the LHC (based on the structure functions obtained in [8]).

The calculation of the W/Z p_T distribution has been a classic problem in QCD. For large p_T, for example $p_T \sim o(m_W)$, the p_T distribution can be reliably computed in perturbation theory, which was done up to NLO in the late '70's and early '80's. A problem arises in the intermediate range $\Lambda_{QCD} << p_T << m_W$, where the bulk of the data is concentrated, because terms of order $\alpha_s(p_T^2) \log m_W^2/p_T^2$ become of order 1 and should included to all orders. At order α_s we have:

$$\frac{1}{\sigma_0}\frac{d\sigma_0}{dp_T^2} \;=\; (1+A)\delta(p_T^2) \;+\; \frac{B}{p_T^2}\log\frac{m_W^2}{p_T^2}_{\;+} \;+\; \frac{C}{(p_T^2)_+} \;+\; D(p_T^2) \tag{95}$$

where A, B, C, D are coefficients of order α_s. The "+" distribution is defined in complete analogy with eq.(91):

$$\int_0^{p_{TMAX}^2} g(z) f(z)_+ dz \;=\; \int_0^{p_{TMAX}^2} [g(z) - g(0)] f(z) dz \tag{96}$$

The content of this at first sight mysterious definition is that the singular "+" terms do not contribute to the total cross-section. In fact for the cross-section the weight function $g(z) = 1$ and we obtain:

$$\sigma \;=\; \sigma_0[(1+A) \;+\; \int_0^{p_{TMAX}^2} D(z) dz] \tag{97}$$

The singular terms, of infrared origin, are present at the non completely inclusive level but disappear in the total cross-section. These singularities are proven to exponentiate and lead to

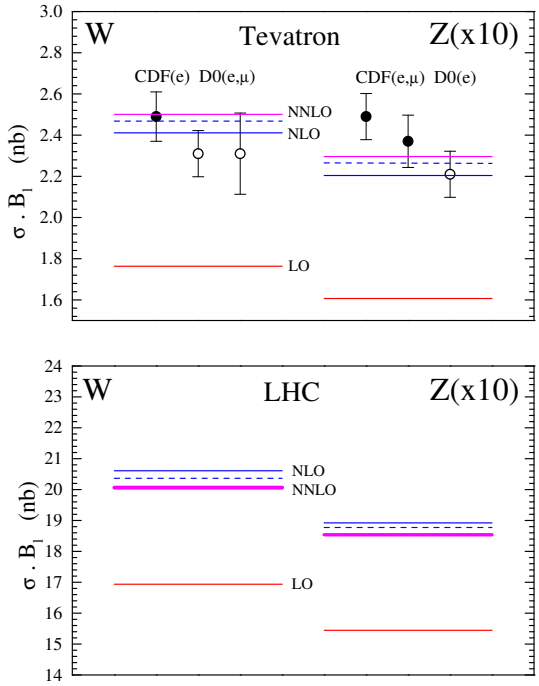

Fig. 18: Data vs. theory for W and Z production at the Tevatron ($\sqrt{s} = 1.8$ TeV) together with the corresponding predictions for the LHC ($\sqrt{s}$= 1.4 TeV)

the following expression:

$$\frac{1}{\sigma_0}\frac{d\sigma_0}{dp_T^2} = \int \frac{d^2b}{4\pi} \exp(-ib\cdot p_T)(1+A)\exp S(b) \tag{98}$$

with:

$$S(b) = \int_0^{p_{TMAX}} \frac{d^2k_T}{2\pi}[\exp ik_T\cdot b - 1][\frac{B}{k_T^2}\log\frac{m_W^2}{k_T^2} + \frac{C}{k_T^2}] \tag{99}$$

At large p_T the LO perturbative expansion is recovered. At intermediate p_T the infrared p_T singularities are resummed (the Sudakov log terms, which are typical of vector gluons, are related to the fact that for a charged particle in acceleration it is impossible not to radiate, so that the amplitude for no soft gluon emission is exponentially suppressed). However this formula has problems at small p_T, for example, because of the presence of α_s under the integral for $S(b)$: presumably the relevant scale is of order k_T^2. So it must be completed by some non perturbative ansatz or an extrapolation into the soft region. All the exercise has been extended to NLO accuracy, where one starts from the perturbative expansion at order α_s^2, and generalises the resummation to also include NLO terms of order $\alpha_s(p_T^2)^2\log m_W^2/p_T^2$. The comparison with the data is very impressive. In Fig. 19 we see the p_T distribution as predicted in QCD (with a number of variants that mainly differ in the approach to the soft region) compared with some recent data from the D0 Collaboration at the Tevatron [10].

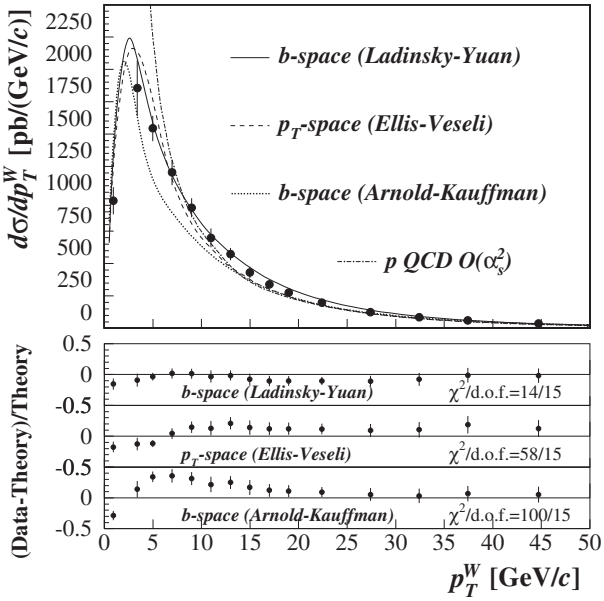

Fig. 19: QCD predictions for the W p_T distribution compared with recent D0 data at the Tevatron ($\sqrt{s} = 1.8$ TeV)

6 MEASUREMENTS OF α_s

The most precise and reliable measurements of $\alpha_s(m_Z^2)$ in the $\bar{M}S$ definition are obtained from e^+e^- colliders (in particular LEP) and from Deep Inelastic Scattering.

6.1 α_s from e^+e^- colliders

The main methods at e^+e^- colliders are: a) Inclusive hadronic Z decay, R_l, σ_h, Γ_Z. b) Inclusive hadronic τ decay. c) Event shapes and jet rates.

As we have seen, for a quantity like R_l we can write a general expression of the form:

$$R_l \;=\; \frac{Z, \tau \to hadrons)}{Z, \tau \to leptons)} \;\sim\; R^{EW}(1 \;+\; \delta_{QCD} \;+\; \delta_{NP}) \;+ ... \tag{100}$$

where R^{EW} is the electroweak-corrected Born approximation, δ_{QCD}, δ_{NP} are the perturbative (logarithmic) and non perturbative (power suppressed) QCD corrections. If we consider measurement at the Z, from R_l only, assuming the standard electroweak theory, one finds [11]:

$$\alpha_s(m_Z) = 0.123 \pm 0.004 \tag{101}$$

Better, one can use all info from R_l, $\Gamma_Z = 3\Gamma_l + \Gamma_h$ and $\sigma_h = 12\pi\Gamma_l\Gamma_h/(m_Z^2\Gamma_Z^2)$. From these observables together one obtains:

$$\alpha_s(m_Z) = 0.120 \pm 0.003 \tag{102}$$

By adding all other electroweak precision electroweak tests (in particular m_W) one finds:

$$\alpha_s(m_Z) = 0.118 \pm 0.003 \tag{103}$$

The final error is predominantly theoretical and is dominated by our ignorance on m_H and from higher orders in the QCD expansion.

We now consider the measurement of $\alpha_s(m_Z)$ from τ decay. R_τ has a number of advantages that, at least in part, tend to compensate for the smallness of $m_\tau = 1.777\ GeV$. First, R_τ is maximally inclusive, more than $R_{e^+e^-}(s)$, because one also integrates over all values of the invariant hadronic squared mass:

$$R_\tau = \frac{1}{\pi}\int_0^{m_\tau^2}\frac{ds}{m_\tau^2}(1-\frac{s}{m_\tau^2})^2 Im\Pi_\tau(s) \tag{104}$$

Analyticity can be used to transform the integral into one on the circle at $|s| = m_\tau^2$:

$$R_\tau = \frac{1}{2\pi i}\oint_{|s|=m_\tau^2}\frac{ds}{m_\tau^2}(1-\frac{s}{m_\tau^2})^2\Pi_\tau(s) \tag{105}$$

Also, the factor $(1-\frac{s}{m_\tau^2})^2$ is important to kill the sensitivity the region $Res = m_\tau^2$ where the physical cut and the associated thresholds are located. Still the quoted result (a combination of ALEPH and OPAL analyses) looks a bit too precise:

$$\alpha_s(m_Z) = 0.1181 \pm 0.0007(exp) \pm 0.003(th) \tag{106}$$

This precision is obtained by taking for granted that corrections suppressed by $1/m_\tau^2$ are negligible. This is because, in the massless theory, the light cone expansion is given by:

$$\delta_{NP} = \frac{ZERO}{m_\tau^2} \ + \ c_4\cdot\frac{< O_4 >}{m_\tau^4} \ + \ c_6\cdot\frac{< O_6 >}{m_\tau^6} \ + \cdots \tag{107}$$

In fact there are no dim-2 Lorentz and gauge invariant operators. For example, $g_\mu g^\mu$ is not gauge invariant. In the massive theory, the ZERO is replaced by light quark mass-squared m^2. This is still negligible if m is taken as a lagrangian mass of a few MeV. But would not at all be negligible, actually would very much affect the result, if it is taken as a constituent mass of order $m \sim \Lambda_{QCD}$. Most people believe the optimistic version. I am not convinced that the gap is not filled up by ambiguities of $0(\Lambda_{QCD}^2/m_\tau^2)$ from δ_{pert}. In any case, one can discuss the error, but it is true and remarkable, that the central value from τ decay, obtained at very small Q^2, is in perfect agreement with all other precise determinations of α_s at more typical LEP values of Q^2.

6.2 α_s from Deep Inelastic Scattering

QCD predicts the Q^2 dependence of $F(x,Q^2)$ at each fixed x, not the x shape. But the Q^2 dependence is related to the x shape by the QCD evolution equations. For each x-bin the data allow to extract the slope of an approximately stright line in $dlogF(x,Q^2)/dlogQ^2$: the log slope. The Q^2 span and the precision of the data are not much sensitive to the curvature, for most x values. A single value of Λ_{QCD} must be fitted to reproduce the collection of the log slopes. For the determination of α_s the scaling violations of non-singlet structure functions would be ideal, because of the minimal impact of the choice of input parton densities. We can write the non-singlet evolution equations in the form:

$$\frac{d}{dt}logF(x,t) \ = \ \frac{\alpha_s(t)}{2\pi}\int_x^1\frac{dy}{y}\frac{F(y,t)}{F(x,t)}P_{qq}(\frac{x}{y},\alpha_s(t)) \tag{108}$$

where P_{qq} is the NLO splitting function. It is clear from this form that, for example, the normalisation of the input density drops away, and the dependence on the input is reduced to a minimum (also there is a single density, while in general there are quark and gluon densities). Unfortunately the data on non-singlet structure functions are not very accurate. If we take

the difference of data on protons and neutrons, $F_p - F_n$, experimental errors add up in the difference and finally are large. The $F_{3\nu N}$ data are directly non-singlet but are not very precise. A determination of α_s from the CCFR data on $F_{3\nu N}$ has led to [12]:

$$\alpha_s(m_Z) = 0.118 \pm 0.006 \tag{109}$$

When one measures α_s from scaling violations on F_2 from e or μ beams, the data are abundant, the errors small but there is an increased dependence on input parton densities and especially a strong correlation between the result on α_s and the input on the gluon density. There are two most complete and accurate derivations of α_s from scaling violations in F_2. In the first analysis, by Santiago and Yndurain [13], the data on protons from SLAC, BCDMS, E665 and HERA are used with NLO kernels plus the NNLO first few moments. The analysis is based on an original method that uses projections on a specially selected basis of orthogonal polynomials. The quoted result is given by:

$$\alpha_s(m_Z) = 0.117 \pm 0.003 \tag{110}$$

A different analysis by Alekhin [14] of a similar collection of proton data from SLAC, BCDMS, NMC and HERA with NLO kernels and a more conventional method leads to

$$\alpha_s(m_Z) = 0.116 \pm 0.003 \tag{111}$$

In both analysis the dominant error is theoretical and could be somewhat larger than quoted.

If we compare these results on α_s from DIS with the findings at the Z, given by eq.(103), we see that the agreement looks perfect. But, in my opinion, the situation of α_s from DIS is not yet completely satisfactory (while it is so for α_s from e^+e^-). The data have shown large fluctuations in the recent past. For example, the original result obtained by combining BCDMS and SLAC data was [15]:

$$\alpha_s(m_Z) = 0.113 \pm 0.005 \tag{112}$$

This low value appeared to be confirmed by the CCFR result from F_2 and F_3 data combined:

$$\alpha_s(m_Z) = 0.111 \pm 0.005 \tag{113}$$

But later the same data were corrected by a new energy calibration performed by the collaboration and the result become:

$$\alpha_s(m_Z) = 0.119 \pm 0.005 \tag{114}$$

So the experimental errors are perhaps larger than quoted and there is a problem for matching the systematics of different experiments. On the theory side the analysis methods are perhaps still not completely optimised.

Summarising: there is very good agreement among many different measurements of α_s (see Fig. 20, [4]). This is a very convincing, quantitative test of QCD. The average value quoted by PDG 2000 is

$$\alpha_s(m_Z) = 0.118 \pm 0.002 \tag{115}$$

The corresponding value of Λ (for $n_f = 5$) is:

$$\Lambda_5 = 209 \pm 24 \; MeV \tag{116}$$

Λ is the scale of mass that finally appears in massless QCD. It is the scale where $\alpha_s(\Lambda)$ is of order 1. Hadron masses are determined by Λ. Actually the ρ mass or the nucleon mass receive little contribution from the quark masses (the case of pseudoscalar mesons is special, as they are the pseudo Goldstone bosons of broken chiral invariance). Hadron masses would be almost the same in massless QCD.

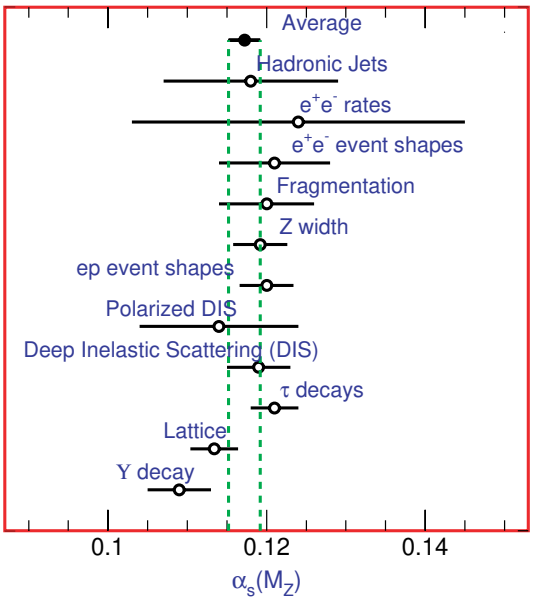

Fig. 20: The PDG (Ref. [4]) compilation of the existing precise measurements of $\alpha_s(M_2)$

7 CONCLUSION

We have seen that perturbative QCD based on asymptotic freedom offers a rich variety of tests and we have described some examples in detail. QCD tests are not as precise as for the electroweak sector. But the number and diversity of such tests has established a very firm experimental foundation for QCD as a theory of strong interactions.

The field is still very much in movement. There are areas of continuous development: I list here some of these domains where work is in progress and which would deserve an expanded discussion.

Higher order calculations: important examples are the effort to complete the 3-loop analytic determination of the splitting functions, and the calculation of 4-jet distributions at NLO in e^+e^- annihilation.

Resummations in problems with 2 (or more) different large scales: if y=scale1/scale2 one needs to resum $(\alpha_s \log^a y)^n$, with $a = 1, 2$, at all orders in n. We have seen an example on the W, Z p_T distribution in pp or $p\bar{p}$ collisions for $\Lambda_{QCD} << p_T << m_W$ where all terms of order $(\alpha_s(p_T^2) \log m_W^2/p_T^2)^n$ must be taken into account. Other examples involve structure functions at small x $((\alpha_s(Q^2) \log 1/x)^n)$ or at $x \sim 1$ $((\alpha_s(Q^2) \log 1/(1-x))^n)$, or thrust distributions near $T \sim 1$ etc.

Renormalons and power suppressed corrections (for an introduction see, for example, Ref [16]).. The QED and QCD perturbative series, after renormalisation, have all their coefficients finite, but it is well known that the expansion does not converge. Actually the perturbative series is not even Borel summable. After Borel resummation for a given process one is left with a result which is ambiguous by terms typically down by $-\exp(-n/b\alpha)$, with n an integer and b the first β function coefficient. In QED these corrective terms are extremely small and not very important in practice. On the contrary in QCD $\alpha = \alpha_s(Q^2) \sim 1/(b \log Q^2/\Lambda^2)$ and the ambiguous terms are of order $(1/Q^2)^n$, that is are power suppressed. The problem arises of the precise relation between the ambiguities of the perturbative expansion and the higher twist corrections, which is a very interesting field of research.

New areas explored by experiment. Particularly interesting physics cases are present in

polarized deep inelastic scattering, or in the phenomenology of structure functions at small x as measured at HERA.

An important domain of activity is the QCD event simulation for the preparation of LHC experiment which poses highly non trivial theoretical and technical problems.

8 APPENDIX: The Formalism of Gauge Theories

We summarize here the definition and the structure of a gauge Yang–Mills theory.

Consider a Lagrangian density $\mathcal{L}[\phi, \partial_\mu \phi]$ which is invariant under a D dimensional continuous group of transformations:

$$\phi' = U(\theta^A)\phi \qquad (A = 1, 2, ..., D) \ . \tag{117}$$

For θ^A infinitesimal, $U(\theta^A) = 1 + ig \sum_A \ \theta^A T^A$, where T^A are the generators of the group Γ of transformations (117) in the (in general reducible) representation of the fields ϕ. Here we restrict ourselves to the case of internal symmetries, so that T^A are matrices that are independent of the space–time coordinates. The generators T^A are normalized in such a way that for the lowest dimensional non-trivial representation of the group Γ (we use t^A to denote the generators in this particular representation) we have

$$\mathrm{tr}(t^A t^B) = \frac{1}{2}\delta^{AB} \ . \tag{118}$$

The generators satisfy the commutation relations

$$[T^A, T^B] = iC_{ABC}T^C \ . \tag{119}$$

In the following, for each quantity V^A we define

$$\mathbf{V} = \sum_A \ T^A V^A \ . \tag{120}$$

If we now make the parameters θ^A depend on the space–time coordinates $\theta^A = \theta^A(x_\mu)$, $\mathcal{L}[\phi, \partial_\mu \phi]$ is in general no longer invariant under the gauge transformations $U[\theta^A(x_\mu)]$, because of the derivative terms. Gauge invariance is recovered if the ordinary derivative is replaced by the covariant derivative:

$$D_\mu = \partial_\mu + ig\mathbf{V}_\mu \ , \tag{121}$$

where V_μ^A are a set of D gauge fields (in one-to-one correspondence with the group generators) with the transformation law

$$\mathbf{V}'_\mu = U\mathbf{V}_\mu U^{-1} - (1/ig)(\partial_\mu U)U^{-1} \ . \tag{122}$$

For constant θ^A, $\mathbf{V}$ reduces to a tensor of the adjoint (or regular) representation of the group:

$$\mathbf{V}'_\mu = U\mathbf{V}_\mu U^{-1} \simeq \mathbf{V}_\mu + ig[\theta, \mathbf{V}_\mu] \ , \tag{123}$$

which implies that

$$V_\mu'^C = V_\mu^C - gC_{ABC}\theta^A V_\mu^B \ , \tag{124}$$

where repeated indices are summed up.

As a consequence of Eqs. (121) and (122), $D_\mu \phi$ has the same transformation properties as ϕ:

$$(D_\mu \phi)' = U(D_\mu \phi) \ . \tag{125}$$

Thus $\mathcal{L}[\phi, D_\mu\phi]$ is indeed invariant under gauge transformations. In order to construct a gauge-invariant kinetic energy term for the gauge fields V^A, we consider

$$[D_\mu, D_\nu]\phi = ig\{\partial_\mu \mathbf{V}_\nu - \partial_\nu \mathbf{V}_\mu + ig[\mathbf{V}_\mu, \mathbf{V}_\nu]\}\phi \equiv ig\mathbf{F}_{\mu\nu}\phi \ , \tag{126}$$

which is equivalent to

$$F^A_{\mu\nu} = \partial_\mu V^A_\nu - \partial_\nu V^A_\mu - gC_{ABC}V^B_\mu V^C_\nu \ . \tag{127}$$

From Eqs. (117), (125) and (126) it follows that the transformation properties of $F^A_{\mu\nu}$ are those of a tensor of the adjoint representation

$$\mathbf{F}'_{\mu\nu} = U\mathbf{F}_{\mu\nu}U^{-1} \ . \tag{128}$$

The complete Yang–Mills Lagrangian, which is invariant under gauge transformations, can be written in the form

$$\mathcal{L}_{\rm YM} = -\frac{1}{4}\sum_A F^A_{\mu\nu}F^{A\mu\nu} + \mathcal{L}[\phi, D_\mu\phi] \ . \tag{129}$$

For an Abelian theory, as for example QED, the gauge transformation reduces to $U[\theta(x)] = \exp[ieQ\theta(x)]$, where Q is the charge generator. The associated gauge field (the photon), according to Eq. (122), transforms as

$$V'_\mu = V_\mu - \partial_\mu\theta(x) \ . \tag{130}$$

In this case, the $F_{\mu\nu}$ tensor is linear in the gauge field V_μ so that in the absence of matter fields the theory is free. On the other hand, in the non-Abelian case the $F^A_{\mu\nu}$ tensor contains both linear and quadratic terms in V^A_μ, so that the theory is non-trivial even in the absence of matter fields.

References

[1] G. Altarelli, Phys. Rep. 81(1982)1.

[2] G. Altarelli, Ann. Rev. Nucl. Part. Sci. 39(1989)357.

[3] G. Altarelli, "The Development of Perturbative QCD", World Scientific, 1994.

[4] Particle Data Group, The Europ. Phys. J. C 15(2000)1.

[5] O.V. Tarasov, A.A. Vladimirov and A. Yu. Zharkov, Phys. Lett. 93B(1980)429.

[6] S.G. Gorishny, A.L. Kataev and S.A. Larin, Phys. Lett. 259B (1991) 144; L. R. Surguladze and M. A. Samuel, Phys. Rev. Lett. 66 (1991) 560.

[7] for a review, see, for example, S. Moch, J. A. M. Vermaseren and M. Zhou, hep-ph/0108033.

[8] A. D. Martin, R. G. Roberts, W. J. Stirling and R. S. Thorne, hep-ph/0110215, hep-ph/0201127.

[9] R. Hamberg, W. L. van Neerven and T. Matsuura, Nucl. Phys. B359 (1991) 343; W. L. van Neerven and E. B. Zijlstra, Nucl. Phys. B382(1992) 11.

[10] The D0 collaboration, hep-ex/0010026.

[11] For up-to-date results see, The LEP Electroweak Group, http://lepewwg.web.cern.ch/LEPEWWG/.

[12] A.L. Kataev, G. Parente and A.V. Sidorov, Nucl.Phys. B573 (2000) 405.

[13] J. Santiago and F.J. Yndurain Nucl.Phys. B563 (1999) 45.

[14] S.I. Alekhin, Phys. Rev. D63 (2001) 094022, Phys. Lett. B519 (2001) 57.

[15] M. Virchaux and A. Milsztajn, Phys. Lett. B274 (1992) 221.

[16] G. Altarelli, Proceedings of the E. Majorana Summer School, Erice, 1995, Plenum Press, ed. by A. Zichichi.